Check for updates

JGR Atmospheres

RESEARCH ARTICLE
10.1029/2021JD035095

Evidence of Recent Active Volcanism in the Balleny Islands (Antarctica) From Ice Core Records

Dieter R. Tetzner[1,2], Elizabeth R. Thomas[1], Claire S. Allen[1], and Alma Piermattei[3]

[1]British Antarctic Survey, Cambridge, UK, [2]Department of Earth Sciences, University of Cambridge, Cambridge, UK, [3]Department of Geography, University of Cambridge, Cambridge, UK

Key Points:

- Evidence from ice cores is used to verify a volcanic eruption in the Balleny islands in 2001 CE, supporting evidence from satellites
- Characterization and timing of microparticles and tephra associated with this eruption provide a chronostratigraphic marker for ice cores

Correspondence to:

D. R. Tetzner,
dietet95@bas.ac.uk

Citation:

Tetzner, D. R., Thomas, E. R., Allen, C. S., & Piermattei, A. (2021). Evidence of recent active volcanism in the Balleny Islands (Antarctica) from ice core records. *Journal of Geophysical Research: Atmospheres*, *126*, e2021JD035095. https://doi.org/10.1029/2021JD035095

Received 17 APR 2021
Accepted 9 NOV 2021

Author Contributions:

Conceptualization: Dieter R. Tetzner, Elizabeth R. Thomas, Claire S. Allen
Formal analysis: Dieter R. Tetzner, Elizabeth R. Thomas, Claire S. Allen, Alma Piermattei
Investigation: Dieter R. Tetzner, Elizabeth R. Thomas, Claire S. Allen
Methodology: Dieter R. Tetzner, Elizabeth R. Thomas, Claire S. Allen
Writing – original draft: Dieter R. Tetzner, Elizabeth R. Thomas, Claire S. Allen
Writing – review & editing: Dieter R. Tetzner, Elizabeth R. Thomas, Claire S. Allen, Alma Piermattei

© 2021. The Authors.
This is an open access article under the terms of the Creative Commons Attribution License, which permits use, distribution and reproduction in any medium, provided the original work is properly cited.

Abstract Volcanism can play a key role in modulating climate; however, a lack of historical records has limited our comprehension of Antarctic volcanism and its role on the cryosphere. Remote sensing can provide insight into active volcanism in Antarctica during the satellite era, although the evidence is often inconclusive. Here, we use independent evidence from ice cores to validate one such potential volcanic eruption from the sub-Antarctic Balleny Islands in 2001 CE. Multiple ice cores from downwind of the eruption site, record elevated input of sulfate, microparticles, and the presence of tephra, coincident with the eruption. In-phase deposition of volcanic products confirmed a rapid tropospheric transport of volcanic emissions from a small-to-moderate, local eruption during 2001. Air mass trajectories demonstrated some air parcels were transported over the West Antarctic ice sheet from the Balleny Islands to ice core sites at the time of the potential eruption, establishing a route for transport and deposition of volcanic products over the ice sheet. The data presented here validate previous remote sensing observations and confirms a volcanic event in the Balleny Islands during 2001 CE. This newly identified eruption provides a case study of recent Antarctic volcanism.

1. Introduction

Antarctica is considered one of the least volcanically active regions on Earth, with the highest number of volcanoes listed as uncertainly active and many others hidden beneath the ice sheet (Hund, 2014). Over 100 volcanoes have been identified in the Antarctic continent and sub-Antarctic Islands (de Vries et al., 2018; LeMasurier et al., 1990) with more than 20 documented in the historical records (Patrick & Smellie, 2013). Among the historically active, just two are frequently monitored by ground-based instruments (Mount Erebus and Deception Island; LeMasurier et al., 1990; Patrick & Smellie, 2013; Smellie et al., 2021), while the others are rarely surveyed due to their extreme isolation. Remote sensing techniques have helped to monitor regional volcanism; however, high detection thresholds and coarse spatial resolution have hindered the capacity of some sensors to accurately identify volcanic activity (Patrick & Smellie, 2013). Moreover, the effects of volcanism can be rapidly obscured in the Antarctic and sub-Antarctic environment due to frequent snowfall and cloud coverage (LeMasurier et al., 1990). Even though Antarctic volcanoes do not present significant direct hazards, their study is important for many areas of research. Mainly, geothermal heat flux estimates (Vogel et al., 2006), ice flow dynamics models (Bingham & Siegert, 2009), and the volcanic effects on the polar climate (Cole-Dai, 2010; Robock, 2000; Sigl et al., 2014). Altogether, the remoteness and inaccessibility of most of the Antarctic volcanoes have strongly limited our knowledge of the Antarctic volcanic activity.

An alternative way to study volcanic activity in Antarctica is the analyses of volcanic tephra (assortment of fragments, from blocks of material to ash, ejected into the air during a volcanic eruption; Kittleman, 1979) preserved in ice core layers. Volcanic eruptions may also emit large amounts of particulate matter and sulfur compounds into the atmosphere. Sulfur compounds are oxidized to sulfuric acid ($H_2SO_4^2$) and travel as particulate aerosols in the atmosphere. Volcanic sulfate aerosols and tephra in the atmosphere can be transported thousands of kilometers from the volcanic source, to be deposited and preserved on polar ice sheets (Koffman et al., 2017). Measurements of sulfate concentrations and electric conductivity (EC) in the ice strata help to detect and quantify past volcanic activity over thousands of years (Cole-Dai, 2010; Cole-Dai et al., 1997). Similarly, the physical and chemical characterization of tephra and cryptotephra (micrometer-sized tephra) embedded in ice layers can record past volcanic activity and fingerprint the source of the volcanic eruptions (Dunbar & Kurbatov, 2011; Narcisi et al., 2019). These methods have been applied to several Antarctic ice cores, providing evidence of past volcanic activity at regional, hemispheric, and global scales (Basile et al., 2001; Fujita et al., 2015; Jiang et al., 2012; Lee et al., 2020; Narcisi et al., 2016; Parrenin et al., 2012; Severi et al., 2012; Udisti et al., 2000).

From a regional perspective, the study of volcanic products preserved in ice cores has contributed to determining the recurrence of explosive volcanic activity in different volcanic groups and provinces around Antarctica (Narcisi et al., 2005, 2010, 2012).

Previous studies have shown that ice cores from the Antarctic Peninsula, Ellsworth Land, and Marie Byrd Land record large-scale and regional explosive volcanic eruptions (Abram et al., 2011; Cole-Dai et al., 1997; Dixon et al., 2004; Dunbar & Kurbatov, 2011; Dunbar et al., 2003; Goodwin, 2013; Koffman et al., 2013; Mulvaney et al., 2012; Palais, 1985; Thomas & Abram, 2016). Most studies have focused on detecting large explosive tropical eruptions (Pinatubo (1991), Agung (1963), Tambora (1815), among others) to establish absolute time markers for ice core chronologies or set tie-points to synchronize different records. Only a few studies document regional volcanism, mostly focused on volcanic activity in Deception Island, off the northern Antarctic Peninsula (Aristarain & Delmas, 1998; Dunbar et al., 2003; Jiankang et al., 1999; Koffman et al., 2013; Mulvaney et al., 2012).

The Balleny Islands are a chain of volcanic islands off the coast of Victoria Land, Antarctica. Sturge Island (1,167 m a.s.l) is the largest and southern-most island in the volcanic chain (LeMasurier et al., 1990). This island is a stratovolcano covered by an icecap with no records of present or past volcanic activity (Hund, 2014). On June 12, 2001 (13:52 UTC), an unusual cloud formation was spotted over Sturge Island by the U.S. National Ice Center using Optical Line Scan Imagery and was still visible, over to the island, on MODIS imagery at 22:45 UTC (Global Volcanism Program, 2001). Satellite imagery analyses determined the cloud was a single feature in the region, reaching a visible extent of 300 km downwind (E-NE), with a maximum cloud top at approximately 6 km and revealed the possible presence of volcanic SO_2 (Global Volcanism Program, 2001). However, the same analyses revealed the absence of ash in the cloud, presenting the satellite imagery data alone as inconclusive to determine if the cloud was produced by a volcanic eruption in Sturge Island (Global Volcanism Program, 2001).

Here, we aim to use ice cores to independently verify the Sturge Island eruption in 2001. We present a detailed study of five ice core glaciochemical and microparticle records from the southern Antarctic Peninsula, Ellsworth Land, and Marie Byrd Land, to validate the occurrence of this eruption. We include the analysis of insoluble particulate material and cryptotephra in the ice cores as evidence for volcanic activity. Forward air mass trajectories are used to track the air masses originating from the Balleny Islands at the time of the potential 2001 eruption. The aim of this study is to provide independent ice core evidence for a 2001 volcanic eruption on Sturge Island. This study is focused on validating a recent volcanic event in the Balleny Islands and does not intend to present a standardized method to detect the occurrence of small volcanic eruptions in Antarctic ice core records.

2. Methods

2.1. Study Sites

Five ice cores from the southern Antarctic Peninsula, Ellsworth Land, and Marie Byrd Land were included in this study (Figure 1; Table 1). The cores were selected due to their location downwind from the Balleny Islands, their retrieval after the 2001 austral winter, their temporal resolution (>10 samples in the youngest year), their regional distribution, and their data availability. Among the five ice cores used in this study, four (GOM, BC, 01–4, WAIS) have been previously published (Table 1). The 140 m Jurassic ice core (JUR) was drilled by the British Antarctic Survey on the English Coast, Southern Antarctic Peninsula during the austral summer 2012/2013. Ice core samples were cut using a bandsaw with a steel blade and then melted using a Continuous Flow Analysis (CFA) system (Rothlisberger et al., 2000) in the ice chemistry lab at the British Antarctic Survey, UK. An ice core chronology was established based on the hydrogen peroxide annual cycle that is assumed to peak during the summer solstice. The top 53.5 m included in this work date back to 1977 CE, with an estimated dating error for the 1977–2013 interval of ±3 months for each year and with no accumulated error. Discrete ice core samples were cut at 5 cm resolution for major ion analysis (including Methanesulphonic Acid (MSA), sodium, and sulfate) with ion chromatography, using a reagent-free Dionex ICS-2500 anion and IC 2000 cation system.

Four ice cores (GOM, JUR, BC, and WAIS) were evaluated over a 30 yr overlapping period (1977–2007 CE) for evidence of a volcanic eruption in the 2001 ice layer (hereafter referred to as 2001L) The ITASE 01-4 ice core, drilled in 2002, was evaluated over a 25 yr overlapping period (1977–2002 CE). Additionally, two previously identified ice core horizons were targeted as examples of well-dated volcanic events recorded in ice core layers. The 1994–1992 CE horizon for the Mount Pinatubo (Philippines, 15.13°N, 120.35°E) and Cerro Hudson (Chile, 45.92°S, 72.97°W) eruption (Pinatubo/Hudson) (1991 CE) (Cole-Dai & Mosley-Thompson, 1999;

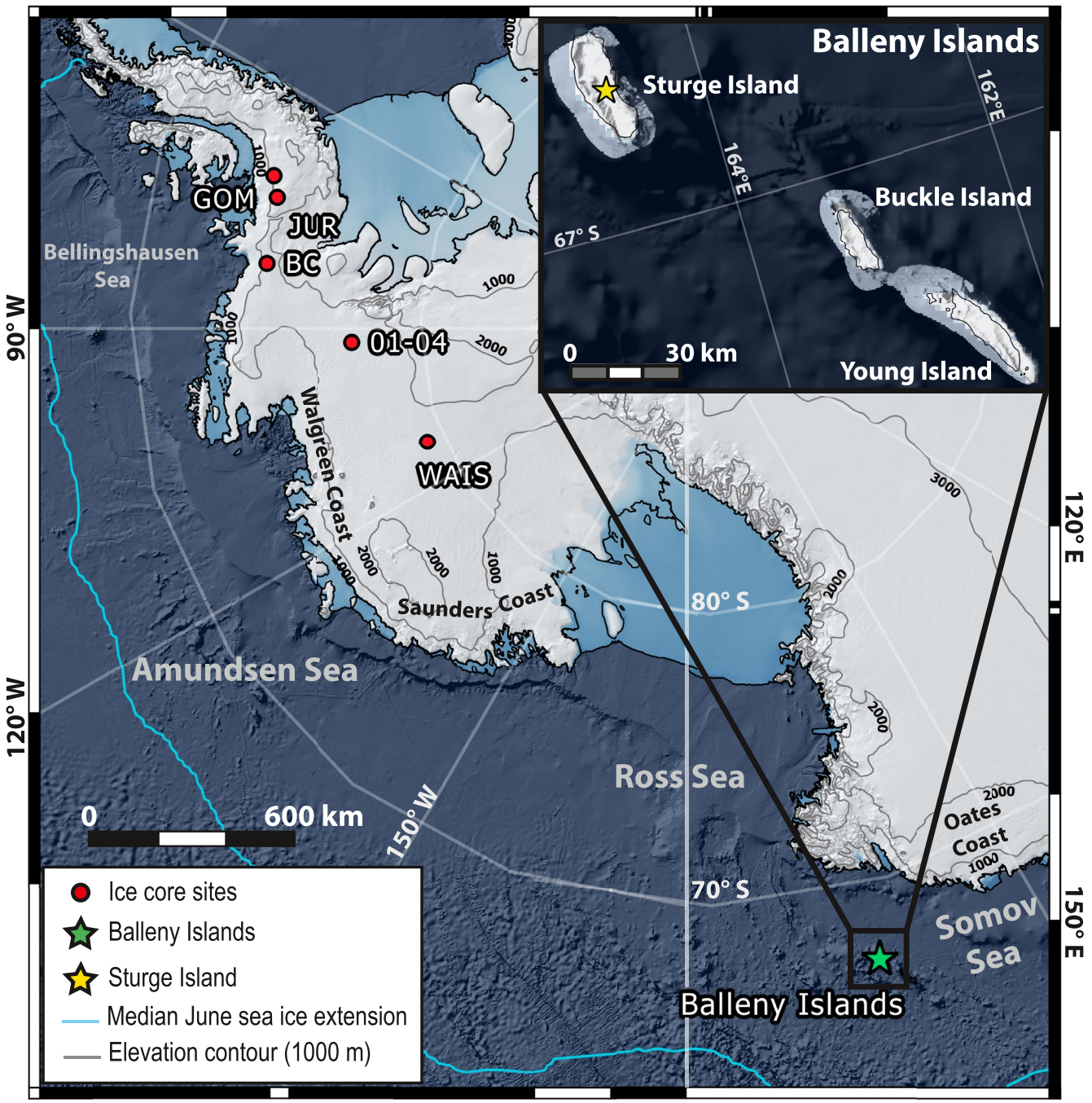

Figure 1. Map showing the ice core sites considered in this study. The red circles show the locations of the five ice core sites. The yellow star shows the location of Sturge Island in the Balleny Islands (green star). The light blue line shows the median June sea ice-extension between 1980 and 2010 CE.

Hoffmann et al., 2020; Jiang et al., 2012; Osipov et al., 2014; Plummer et al., 2012; Schwanck et al., 2017; Thoen et al., 2018; Zhang et al., 2002) and the 1984–1982 CE horizon for the El Chichón eruption (1982 CE) (Mexico, 17.36°N, 93.22°W) (Jiang et al., 2012; Plummer et al., 2012; Thoen et al., 2018; Traufetter et al., 2004). Both eruptions are observed in younger ice core horizons because of the lagged deposition of volcanic sulfates over the Antarctic ice sheet after large low-latitude eruptions (Cole-Dai et al., 1997). All ages presented in this work are based on the ice chronologies reported for each core (Table1).

Table 1
Summary of Each Ice Core Geographical Location and Main Features of the Data Sets Analyzed in This Study

Core name	Abbr.	Long	Lat	Elevation (m a.s.l.)	Year drilled (CE)	Depth interval (m)	Sample resolution (m)	Ice chronology
Gomez	GOM	−70.36	−73.59	1,400	2007	0–45.48	0.02	Thomas et al. (2008)
Jurassic	JUR	−73.06	−74.33	1,139	2013	10.14–53.5	0.05	This work
Bryan Coast	BC	−81.67	−74.49	1,177	2011	4.41–28.45	0.05	Thomas et al. (2015)
ITASE 01-4	01-44	−92.25	−77.61	1,483	2002	0–16.56	0.03	Mayewski and Dixon (2005)
WAIS Divide	WAIS	−112.09	−79.47	1,797	2007	0–12.50	0.03	Sigl et al. (2016)

Note. Abbr: Abbreviation.

2.2. Sulfate Concentration Analyses

Sulfate from volcanic eruptions is superimposed over the background sulfate. This background signal includes organic sulfur compounds, such as dimethyl sulfide (DMS), from marine biogenic emissions (Castellano et al., 2004; Cole-Dai et al., 2000; Dixon et al., 2004; Maupetit & Delmas, 1992; Nardin et al., 2020), with a smaller contribution from sea salt aerosols. Even though the background sulfate is temporally variable, it can be assumed as relatively constant in the last centuries (Castellano et al., 2004; Kreutz et al., 1999, 2000; Traversi et al., 2002). While volcanic sulfate can clearly be identified in continental Antarctic ice cores, the high biogenic background at low elevation coastal sites makes detection more difficult. In particular, the accurate detection of small and moderate volcanic events depends on how the background sulfate is quantified and what volcanic detection threshold is set (Budner & Cole-Dai, 2003; Castellano et al., 2004; Cole-Dai et al., 1997). Several methods have been proposed (Castellano et al., 2004; Cole-Dai et al., 1997; Gautier et al., 2016; Traufetter et al., 2004) based on the evaluation of a background sulfate representative value (m) and its standard deviation (σ) to establish a threshold ($m + 2\sigma$). Sulfate peaks above this threshold are considered indicative of volcanic activity.

In this work, the background signal is evaluated in the total sulfate concentration (SO_4^{2-}) and the non-sea salt sulfate flux ($nssSO_4^{2-}$-flux; Cole-Dai et al., 1997). The $nssSO_4^{2-}$-flux was calculated using Equations 1 and 2 (Wagenbach et al., 1998), using sodium (Na^+) as the reference ion (Castellano et al., 2004; Dixon et al., 2004; Jiang et al., 2012; Li et al., 2012; Osipov et al., 2014; Ren et al., 2010). The analysis of the $nssSO_4^{2-}$-flux was incorporated because it facilitates the detection of small and moderate volcanic signals (Cole-Dai et al., 1997; Zhang et al., 2002). However, we note that the occurrence of extreme precipitation events at coastal sites (Turner et al., 2019) may reduce the reliability of the flux calculations. In the absence of sulfate data from the GOM ice core, the total sulfur (S_{tot}) and non-sea salt sulfur flux (nssS-flux) were used for calculations:

$$\left[\mathrm{nssSO_4^{2-}}\right] = \left[\mathrm{SO_4^{2-}}\right] - 0.253 * \left[\mathrm{Na^+}\right] \quad (1)$$

$$\mathrm{nssSO_4^{2-}\ flux} = \left[\mathrm{nssSO_4^{2-}}\right] * \text{water accumulation} \quad (2)$$

To detect potential volcanic eruptions from elevated SO_4^{2-} and $nssSO_4^{2-}$-flux, we applied the method originally proposed by Castellano et al. (2004). This method was selected over other methods (Cole-Dai et al., 1997; Traufetter et al., 2004) because it considers the log-normal distribution of the sulfate data. The use of log-normal statistics in sulfate analyses has been proven to clearly differentiate between volcanic sulfate and background sulfate (Castellano et al., 2004). To calculate the background sulfate, new data sets were generated after excluding individual ice core horizons from well-known volcanic eruptions between 2007 and 1977 CE (e.g., Pinatubo/Hudson (1991 CE) and El Chichón (1982 CE)). After excluding these horizons, the background and its variability were estimated at each sample point by calculating in the log domain, the mean and standard deviation of a 20% weighted curve fit centered on each sample point (10% weighted curve fit for the shorter 01-4 ice core). The applied curve fit roughly corresponds to a 6-year running mean (approximately 3-year span for 01-4 ice core), ensuring sulfate annual cycle is effectively removed from the background sulfate signal. To identify samples with a potential volcanic influence, the SO_4^{2-} and $nssSO_4^{2-}$-flux had to exceed the background signal (m) by two times the standard deviation ($>2\sigma$-peak). This threshold ensured 95.5% of the random background variability was excluded. SO_4^{2-} and $nssSO_4^{2-}$-flux $> 2\sigma$-peaks were classified based on the number of data points exceeding the threshold (single point (=1) or multiple points (>1)). The method applied in this study assumes that in the

absence of inputs from large volcanic and anthropogenic sources (negligible in Antarctica), the sulfate concentration in the snow comprises inputs from regional background sulfate emissions, not controlled by a dominant source region or transport and deposition processes (Cole-Dai et al., 1997). S_{tot} and nssS-flux from GOM were analyzed using the same method applied for SO_4^{2-} and $nssSO_4^{2-}$-flux detection analyses, respectively.

As previously stated, one of the main sources of background sulfate is DMS from marine biogenic emissions. The oxidation of DMS in the atmosphere produces MSA, a chemical compound widely studied in ice core records because of its link to marine biogenic emissions in the Southern Ocean (Abram et al., 2010, 2013; Criscitiello et al., 2013; Curran et al., 2003; Thomas et al., 2016). The MSA records available for GOM, JUR, and BC ice cores are included to assess whether the SO_4^{2-}>2σ-peaks identified in the 2001L were influenced by increased marine biogenic emissions. MSA records for WAIS and 01-4 ice cores were not available.

Volcanic sulfate fluxes (VSF) were calculated for two of the targeted periods (2001L and 1992–1994 CE). The 1984–1982 CE horizon for the El Chichón eruption (1982 CE) was not included due to the lack of >2σ-peaks in the $nssSO_4^{2-}$-flux profiles. To calculate the VSF, the background $nssSO_4^{2-}$-flux was subtracted from the sample $nssSO_4^{2-}$-flux on each volcanic event identified (>2σ-peak). Therefore, the total flux for a volcanic event is the sum of all the residuals of $nssSO_4^{2-}$-flux samples > $m + 2\sigma$ from the corresponding layers (Jiang et al., 2012). Where elevated $nssSO_4^{2-}$-flux does not exceed the detection threshold ($m + 2\sigma$), the VSF was calculated as the sum of $nssSO_4^{2-}$-flux residuals within the depth interval where an SO_4^{2-}>2σ-peak was identified. To compare the 2001L VSF among different ice cores, the 2001L $nssSO_4^{2-}$-flux was normalized against the $nssSO_4^{2-}$-flux of the well-documented Pinatubo/Hudson eruption (Cole-Dai et al., 1997). Due to the different parameters measured in GOM (S_{tot} and nssS-flux), this ice core was excluded from the VSF calculations.

2.3. Physical Properties Analyses

The EC signal recorded in ice is controlled by soluble impurities that originate mostly from sea salt, biomass burning, and volcanic eruptions, and is strongly correlated with acidity (Mulvaney, 2013). EC measurements from four ice cores were included in this study (only available at GOM, JUR, BC, and WAIS) as an additional data set to test the presence of volcanic products. EC was analyzed in different labs using an Amber Science flow-through meter connected to a continuous ice core melter system. EC data presented a log-normal distribution. Therefore, data treatment and calculations were performed using log-normal statistics. The background conductivity, its variability and the establishment of an excess conductivity detection threshold were calculated following the same method presented in Section 2.2 for SO_4^{2-} and $nssSO_4^{2-}$-flux.

2.4. Forward Trajectory Analyses

Forward trajectory analysis is used to examine the pathways of air masses passing over the Balleny Islands and their potential transit over the ice core sites during the deposition of the 2001L. The National Oceanic and Atmospheric Administration's Hybrid Single-Particle Lagrangian Integrated Trajectory model (Draxler & Hess, 1998; Stein et al., 2015) was used to calculate three-dimensional air parcel pathways under isobaric conditions (2.5° latitude-longitude resolution). Trajectories were calculated starting from the Balleny Islands for a 30 hr interval, 15 hr before, and 15 hr after the first evidence of possible volcanic activity (13:52 UTC on June 12, 2001). Forward trajectories were initiated every hour for up to 10 days using the NCEP/NCAR Reanalysis archives (1948 - present) with three starting elevations: 1,000, 1,500, and 2,000 m above the sea level (a.s.l.). These elevations were selected because of their proximity to the summit of Sturge Island (1,167 m a.s.l), from where a potential volcanic plume could have been emitted. For comparison, trajectories were classified into three groups based on their starting time relative to the first image (Im) evidence of the unusual cloud formation over Sturge Island: pre-Im evidence, first-Im evidence, and post-Im evidence.

2.5. Microparticle Analyses

Microparticle concentration (MPC) and Particle size distributions (PSD) were measured in the JUR and WAIS ice cores. The latter corresponds to the WAIS Divide deep ice core, WDC06A (Kreutz et al., 2011, 2015). MPC from the WDC06A was measured using a flow-through Klotz Abakus laser particle counter connected to a continuous ice core melter system at the University of Maine (Breton et al., 2012). Particles were measured

in 31 size channels, spanning 1–15 μm diameter. Similarly, MPC from the JUR ice core was measured using a flow-through Klotz Abakus laser particle counter connected to a continuous ice core melter system at the British Antarctic Survey. Particles were measured in 23 size channels spanning 0.9–12 μm diameter. MPC data sets presented a log-normal distribution. Therefore, data treatment and calculations were performed using log-normal statistics. To assess whether a MPC peak in the data set could be influenced by volcanic activity, the microparticle background concentration and its variability were calculated. A detection threshold was set following the same guidelines presented in Section 2.2 for sulfate analyses. The JUR dust record is presented with a 4 m gap, due to problems in the data acquisition between 43.6 and 47.6 m deep.

PSD were obtained by calculating the ratio of total volume of insoluble dust contained within each size bin and the derivative of the volume with respect to the natural logarithm of the particle diameter for each bin (dV/dlnD), as presented in Koffman et al. (2014). Three individual ice core horizons were targeted to characterize their PSD: The 2001 ice core horizon (2001L), Pinatubo/Hudson eruption (1991 CE), and El Chichón eruption (1982 CE). To determine if the targeted horizons differ from the background particle size of atmospheric dust, the PSD for the 1977–2007 CE period was calculated as the average PSD after removing the three targeted horizons. For PSD analyses, the mode particle diameter was used as a representative statistic of the volume distribution (Koffman et al., 2014; Ruth et al., 2003).

Microscopy analyses of microparticles were included to determine whether any of the particles present in the 2001 CE horizon were cryptotephra shards. For this, ice samples of 200 mL, from the 2001L of the JUR and GOM ice cores, were melted and filtered. Samples were melted using a CFA system (Rothlisberger et al., 2000) in the ice chemistry lab at the British Antarctic Survey, UK. Meltwater from the CFA waste lines was collected in new bottles then filtered through 13 mm diameter, 1.0 μm pore size Whatman™ Polycarbonate membrane filters, inside clean polypropylene Swinnnex™ filter holders. Filters were mounted onto aluminum stubs for analyses on a scanning electron microscope (SEM) at the Earth Sciences Department of the University of Cambridge. Filters were imaged on a Quanta-650F using back scattered electrons on a low-pressure mode. Each filter was imaged at x800 magnification for cryptotephra identification and physical characterization, following the analysis strategy presented in Tetzner et al. (2021). Two additional samples from the 2001L of the JUR ice core were melted in a class-100 clean room, then centrifuged (6 min at 1,200/1,600 rpm) and decanted successively until samples were concentrated in 2–5 mL fluid. The 2–5 mL sample liquid was homogenized, pipetted onto a single coverslip (22 × 40 mm), dried in an isolated drying cupboard, and then mounted onto a single microscope slide using Norland optical adhesive 61 (refractive index 1.56). Each microscope slide was scanned for the presence of cryptotephra shards.

3. Results

We structure our evidence in the following order, based on their merit as an indicator for this volcanic eruption. (a) Sulfate, a commonly used proxy for past volcanism in continental Antarctic ice cores but less suitable at low elevation and coastal sites where background biogenic sulfur is high. (b) EC, a secondary parameter commonly used to identify volcanic activity. (c) Microparticle concentration (MPC) and size distribution dependent on distance from the source. (d) Cryptotephra, only produced during volcanic eruptions. Each indicator is supported by air-mass trajectory analysis, demonstrating the feasibility that their source corresponds to the Sturge Island eruption in 2001.

3.1. Geochemical Analyses

3.1.1. Sulfate Concentration Profiles

For each core, numerous SO_4^{2-} peaks were identified (GOM (9), JUR (7), BC (6), WAIS (3), and 01–4 (14)) as exceeding the detection threshold ($m + 2\sigma$; Figure 2). The most prominent were almost exclusively associated with the target intervals with volcanic activity (2001, 1994–1992, and 1984–1982). Table 2 presents the main features for each of those peaks.

The 2001L present the most prominent SO_4^{2-}>2σ-peaks during the 1977–2007 CE period, all of them presenting an order of magnitude increase above the background. SO_4^{2-}>2σ-peaks in the 2001L are characterized either by a sharp peak during mid-2001 (GOM, JUR, BC, and 01-4) or by a wide 2001/2000 austral summer peak (WAIS).

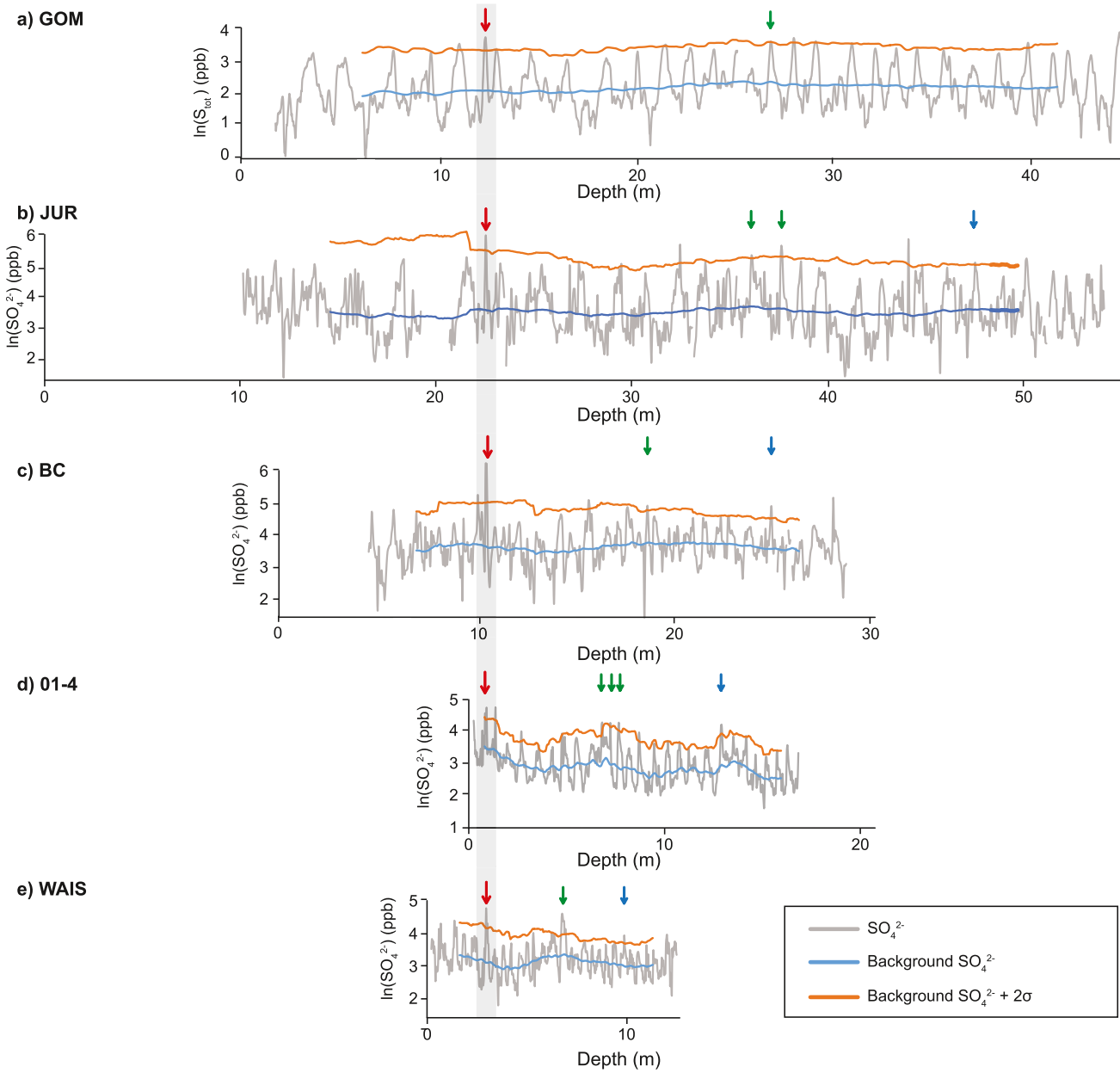

Figure 2. SO_4^{2-} profiles of the depth intervals corresponding to the 1977–2007 CE period for the five ice cores considered in this study. Red arrows indicate peaks above the detection threshold in the 2001 CE ice core layer. Green arrows indicate peaks above the detection threshold in the 1994–1992 CE ice core layer. Blue arrows indicate peaks above the detection threshold in the 1984–1982 CE ice core layer. The gray band highlights the 2001 CE ice core layer.

The SO_4^{2-}>2σ-peaks identified within the 1994–1992 CE ice core layer are characterized by single (GOM, BC, and WAIS) or multiyear sulfate increases (JUR and 01-4) during the austral summer 1991/1992 CE or 1992/1993 CE. SO_4^{2-}>2σ-peaks identified within the 1984–1982 CE ice core layer are consistently smaller than the peaks identified in the other targeted periods and are characterized by a single increase in the SO_4^{2-} concentration during the austral summer 1983/1984 CE.

3.1.2. nssSO_4^{2-}-Flux Profiles

Twenty peaks were identified exceeding the nssSO_4^{2-}-flux detection threshold (nssSO_4^{2-}-flux > 2σ): GOM (8); JUR (2); BC (1); WAIS (2) and 01-4 (7) (Figure 3). All peaks had been previously identified as SO_4^{2-}>2σ-peaks (Figure 2). Among the nssSO_4^{2-}-flux > 2σ-peaks detected, eight occurred within the targeted periods. Table 2 presents the main features for each of these eight peaks.

Table 2
Summary of the Main Features of SO_4^{2-} and nssSO_4^{2-}-Flux >2σ-Peaks Above the Detection Threshold Within the Targeted Periods (2001, 1992–1994, 1982–1984 CE)

Core	Depth interval of excess sulfate (m)	Year in ice chronology (CE)	Data points above the threshold
SO_4^{2-}			
GOM	12.16–12.44	2001	>1
	26.52–26.98	1991/1992	>1
JUR	22.30–22.41	2001	1
	35.64–36.34	1992/1993	>1
	37.19–37.49	1991/1992	>1
	46.90–47.20	1982/1983	1
BC	10.25–10.4	2001	>1
	18.34–18.54	1992/1993	1
	24.54–24.74	1982/1983	>1
01-4	0.56–0.7	2001	>1
	6.46–6.99	1992/1993	>1
	7.34–7.59	1991/1992	>1
	12.55–12.73	1983/1984	>1
WAIS	2.72–2.93	2000/2001	>1
	6.60–6.93	1992/1993	>1
	9.66–9.97	1983	1
nssSO_4^{2-}-flux			
GOM	26.52–26.98	1991/1992	>1
JUR	37.19–37.49	1991/1992	1
01-4	0.56–0.7	2001	>1
	6.46–6.99	1992/1993	>1
	12.55–12.73	1983/1984	>1
WAIS	2.72–2.93	2000/2001	1
	6.60–6.93	1992/1993	>1

The most consistent and prominent nssSO_4^{2-}-flux > 2σ-peaks were identified in the 1993–1992 CE ice core layers. The 2001L exhibited nssSO_4^{2-}-flux > 2σ-peaks in WAIS and 01-4. The 1982–1984 CE period was represented only by a single nssSO_4^{2-}-flux > 2σ-peak in the 01-4 core during the austral summer 1983/1984 CE.

3.1.3. Methanesulphonic Acid (MSA) Measurements

MSA profiles for JUR and BC from 2001L presented prominent peaks of >35 ppb indicative of spring/summer periods and a minimum <5 ppb, denoting the autumn/winter interval. The GOM MSA profile exhibits peaks of >15 ppb indicative of spring/summer and slightly smaller, isolated MSA events that correlate with autumn/winter timing for example, at 11.71 and 12.20 m.

3.1.4. Volcanic Sulfate Flux

The net VSF for 2001L and 1993–1992 CE were calculated (Table 3). The VSF ratio (2001L:1993–1992) exhibited a spatial gradient with higher values (>0.42) for ice cores from Ellsworth Land-Marie Byrd Land (WAIS, O1-4) and considerably lower values (<0.03) for ice cores from the southern Antarctic Peninsula (BC, JUR & GOM).

3.2. Electrical Conductivity (EC) Profiles

EC profiles from four ice cores (GOM, JUR, BC, and WAIS) were examined during the 1977–2007 CE period (Figure 4). In the GOM EC profile, 11 peaks were identified exceeding the conductivity threshold (EC > 2σ-peak). The most prominent peak identified at 12.24 m (0.898 μS s^{-1}), 24.22 m (0.249 μS s^{-1}), and 34.12 m (0.335 μS s^{-1}), corresponding to years 2001, 1993, and 1986 CE. In the JUR EC profile, 24 EC > 2σ-peaks were identified, with the most prominent found at 18.32 m (3.21 μS s^{-1}) and 22.38 m (1.5 μS s^{-1}), corresponding to 2003 and 2001 CE. In the BC EC profile, 14 EC > 2σ-peaks were identified, the most prominent at 10.28 m (0.701 μS s^{-1}), 15.52 m (0.385 μS s^{-1}) and 26.2 m (0.254 μS s^{-1}) corresponding to 2001, 1996, and 1982 CE. In the WAIS EC profile, eight EC > 2σ-peaks were identified, the most prominent occurring at 1.33 m (0.167 μS s^{-1}), 2.82 m (0.163 μS s^{-1}), 3.07 m (0.167 μS s^{-1}) and 5.36 m (0.150 μS s^{-1}), corresponding to years 2003, 2001, 2000, and 1994 CE. Three of the EC > 2σ-peaks were common to all four sites corresponding to the years 2003, 2001, and 1994–1993. The 2001 peak was among the most prominent EC > 2σ-peaks in each EC profile (Figure 4).

3.3. Microparticle Analyses

3.3.1. Microparticle Concentration (MPC)

The MPC (particles per mL – p mL^{-1}) was examined during the 1977–2007 CE period (Figures 5a and 5b). In WAIS, 10 peaks exceeded the MPC threshold. The most prominent peaks corresponding to the 1991–1992 CE period (6.78–6.96 m, 4,257 p mL^{-1}) and smaller peaks corresponding to 1982 and 2001–2000 CE (2.84 m, 2915 p mL^{-1}). In JUR, nine peaks were identified. The most prominent peaks corresponding to 1991–1992 CE (37.38 m, 6,510 p mL^{-1}) with smaller peaks identified corresponding to 1982 and 2001 CE.

3.3.2. Particle Size Distribution (PSD)

The volume concentration parameter (dV/dlnD) of insoluble dust was calculated in WAIS and in JUR for several particle diameters to obtain the particle size distribution (PSD) (Figures 5c and 5d). In the WAIS core, the background PSD (1977–2007 CE) presented a steady increase in concentration with increasing particle diameter (1.3–5.7 μm), followed by a constant decrease for the coarser particles (5.7–15 μm). Similar distributions were

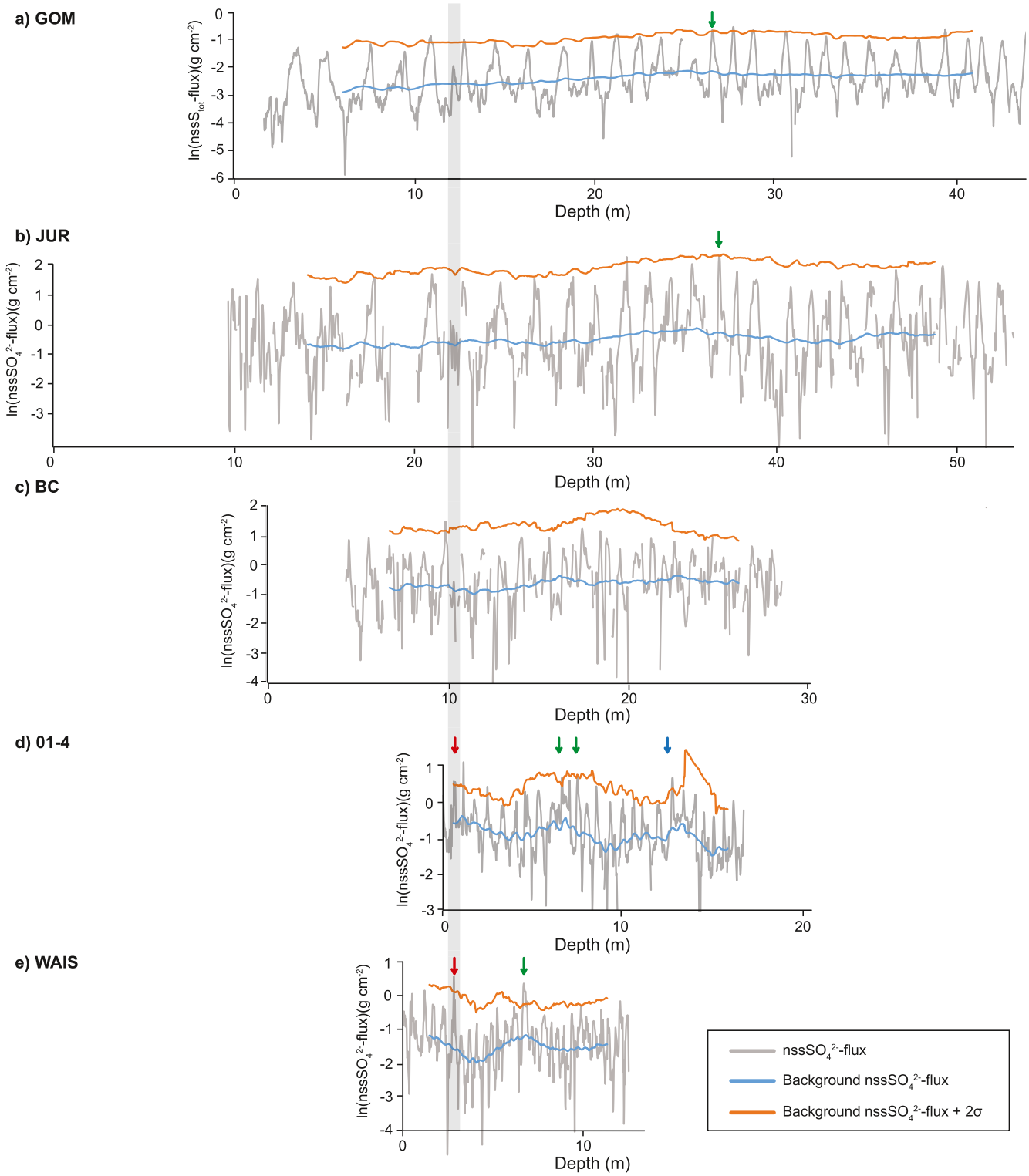

Figure 3. nssSO$_4^{2-}$-flux profiles of the depth interval corresponding to the 1977–2007 CE period for the five ice cores considered in this study. Red arrows indicate peaks above the detection threshold in the 2001 CE ice core layer. Green arrows indicate peaks above the detection threshold in the 1994–1992 CE ice core layer. Blue arrows indicate peaks above the detection threshold in the 1984–1982 CE ice core layer. The gray band highlights the 2001 CE ice core layer.

Table 3
Volcanic Sulfate Fluxes for the 2001 and 1993–1992 Ice Core Layers

Core	VSF (2001L) (g cm^{-3})	VSF (1993–1992 CE) (g cm^{-3})	VSF ratio
Jurassic	0.62	22.77	0.03
Bryan Coast	0.14	5.12	0.03
01-4	1.98	4.64	0.43
WAIS	3.77	8.13	0.46

observed in the three target horizons, except for a notable increase in the coarsest particles (10–12 μm). Despite the similarities, the PSD for Pinatubo/Hudson (1991 CE) and 2001L exhibited considerably higher volume concentration values, up to four-times higher than the background, with PSDs that were completely detached from the background PSD. Likewise, the PSD for El Chichón exhibited higher than background volume concentration values in the finer particles (3.0–5.1 μm). Additional discrepancies were observed in the mode particle diameter. Whilst similar mode diameters were obtained in the background (5.7 μm), Pinatubo/Hudson (5.7 μm) and El Chichón (5.1 μm), the 2001L presented a considerably higher mode particle diameter (10 μm) (Figure 5c).

In the JUR core, the background PSD (1977–2007 CE) presented a steady increase in the volume concentration with increasing particle diameter (1.0–6.0 μm), followed by a slight decrease for the coarser particles (8–12 μm). The three targeted horizons exhibited slightly different distributions. The PSD for El Chichón exhibited a similar distribution and volume concentration to the background. However, the El Chichón PSD presented a comparatively higher volume concentration in the finer particles (3.0–6.0 μm), not identified in the background PSD. The PSD for Pinatubo/Hudson and 2001L present similar distributions with volume concentrations up to an order of magnitude higher than the background. However, the PSD for Pinatubo/Hudson displays a sharp decrease after reaching its highest particle diameter (D) value at $D = 6$ μm, while the PSD for 2001L reaches a steady volume concentration value above $D = 8$ μm. The mode particle diameters for Pinatubo/Hudson (1991 CE) and El Chichón (1982 CE) matched the mode particle diameter of the background (6 μm). Unlike the other targeted horizons, the 2001L presented a higher mode particle diameter (8 μm).

3.3.3. Microscopy Analyses

Two filters containing insoluble particulate material from the 2001L of JUR were analyzed for microparticle characterization (Figure 5e). Seventy particles were identified as cryptotephra shards with a mean size of 19.3 ± 8.7 μm (sizes ranging from 7 to 47 μm). Similarly, two filters containing insoluble particulate matter from the 2001L of GOM were analyzed. Ten particles were identified as cryptotephra shards (Figure 5f) with a mean size of 12.9 ± 3.9 μm (sizes ranging from 7 to 20 μm). Most of the cryptotephra shards identified in both sites (JUR and GOM) were characterized by angular morphologies and concave features (vesicles) without evidence of alteration or corrosion. The cryptotephra shards are cuspate, platy with sharp edges and few with open vesicles and some with butterfly shape. Microscope slides from the 2001L of JUR contained 10 cryptotephra shards with a mean size of 21 μm and exhibiting platy and cuspate textures with round vesicles (Figure 5g).

3.4. Air Mass Trajectories

Forward trajectory analyses showed most of the air masses passing over the Balleny Islands on the June 12, 2011 remained within the Southern Ocean for several days, mainly over the Somov, Ross, Amundsen, and Bellingshausen Seas (Figure 6). Trajectories show air masses were predominantly traveling over the June sea-ice zone, with short periods (<72 h) of transit either over the Antarctic coast (<1,000 m a.s.l) or over the ice sheet (>1,000 m a.s.l.).

After leaving the Balleny Islands, all air masses moving at 1,000 m a.s.l. (Figure 6a) transited over the Oates Coast, some of them reaching Saunders Coast in Marie Byrd Land (See Figure 1 for geographical references). A similar pattern is present in air masses moving at 1,500 m a.s.l. (Figure 6b), where most trajectories transit over the same regions, but some also reach the Walgreen Coast, next to the Amundsen Sea Embayment. Air masses over 2,000 m a.s.l. (Figure 6c) depict a different path with most trajectories moving north toward lower latitudes and only some of them traveling back south, over the ice sheet in Marie Byrd Land, Ellsworth Land, and the southern Antarctic Peninsula. These trajectories passing over Ellsworth Land and the southern Antarctic Peninsula describe the only air masses reaching four of the ice core sites (GOM, JUR, BC, 01-4). These five trajectories represent the paths followed by air masses passing over the Balleny Islands at: 12:00, 13:00, 14:00, 23:00 UTC on the June 12, 2011 and at 02:00 UTC on the June 13, 2001. After leaving the Balleny Islands, four of these trajectories (12:00, 13:00, 14:00, and 23:00 UTC) were transported E-NE and then North, leaving the Southern Ocean and reaching ~43°S. Then they were transported back over the Southern Ocean southwards to the continent. The

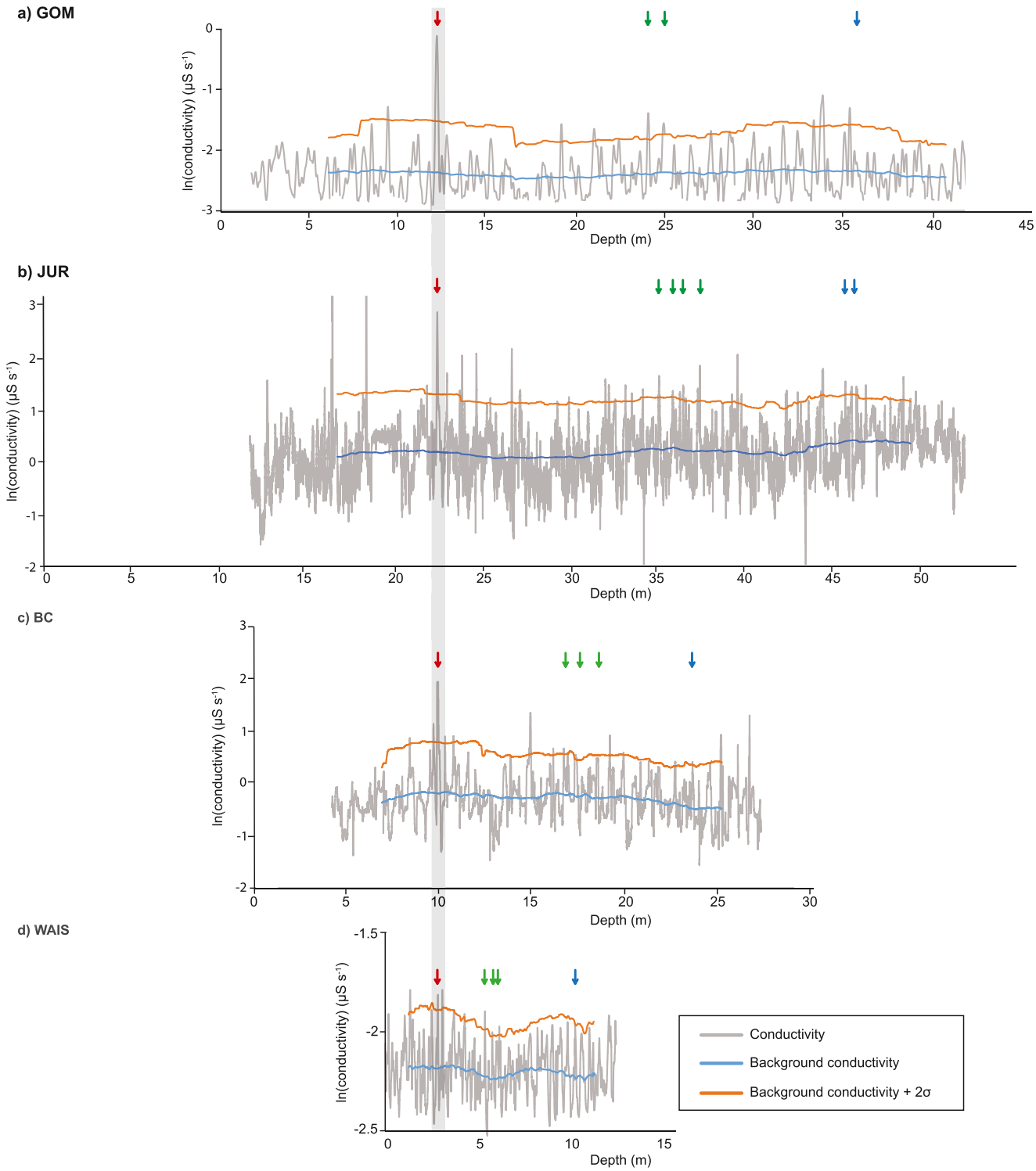

Figure 4. EC profiles for GOM, JUR, BC, and WAIS for the depth interval corresponding to the 1977–2007 CE period. Red arrows indicate peaks above the detection threshold ($>m + 2\sigma$) in the 2001 CE ice core layer. Green arrows indicate peaks above the detection threshold in the 1994–1992 CE ice core layer. Blue arrows indicate peaks above the detection threshold in the 1984–1982 CE ice core layer. The gray band highlights the 2001 CE ice core layer.

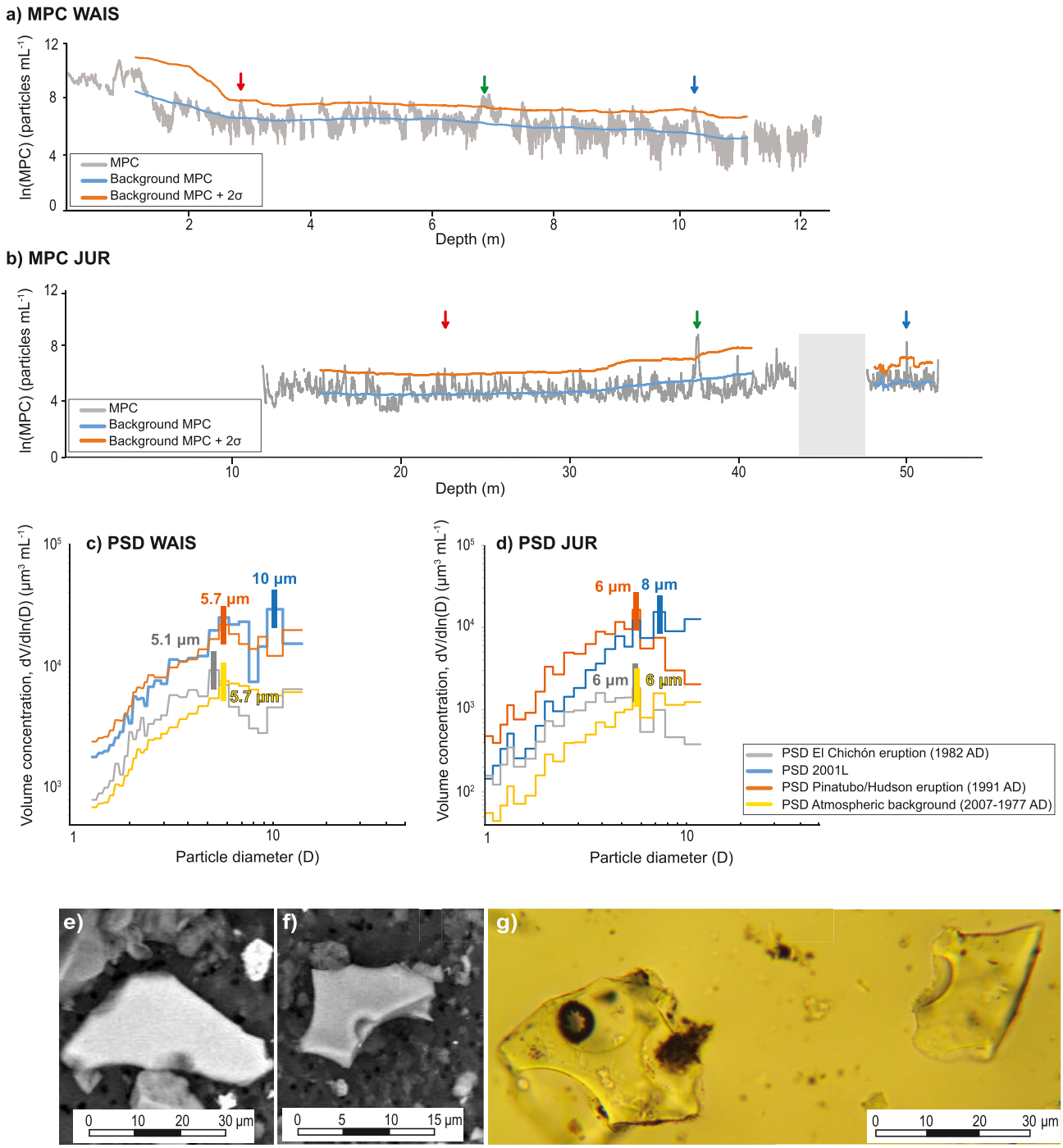

Figure 5. Microparticle analyses from WAIS and JUR ice cores. (a) MPC for the depth interval corresponding to the 1977–2007 CE period from the WAIS ice core. (b) MPC for the depth interval corresponding to the 1977–2007 CE period from the Jurassic ice core. Red arrows indicate peaks above the detection threshold in the 2001 CE ice core layer. Green arrows indicate peaks above the detection threshold in the 1994–1992 CE ice core layer. Blue arrows indicate peaks above the detection threshold in the 1984–1982 CE ice core layer. The gray band indicates a gap in the dust record. (c) PSD curves from the WAIS ice core. (d) PSD curves from the Jurassic ice core. (e and f) show SEM micrographs of cryptotephra shards identified in the 2001 ice core layer from JUR and GOM ice cores respectively. (g) Light microscope micrograph of cryptotephra shards identified in the 2001 CE ice core layer from Jurassic ice core.

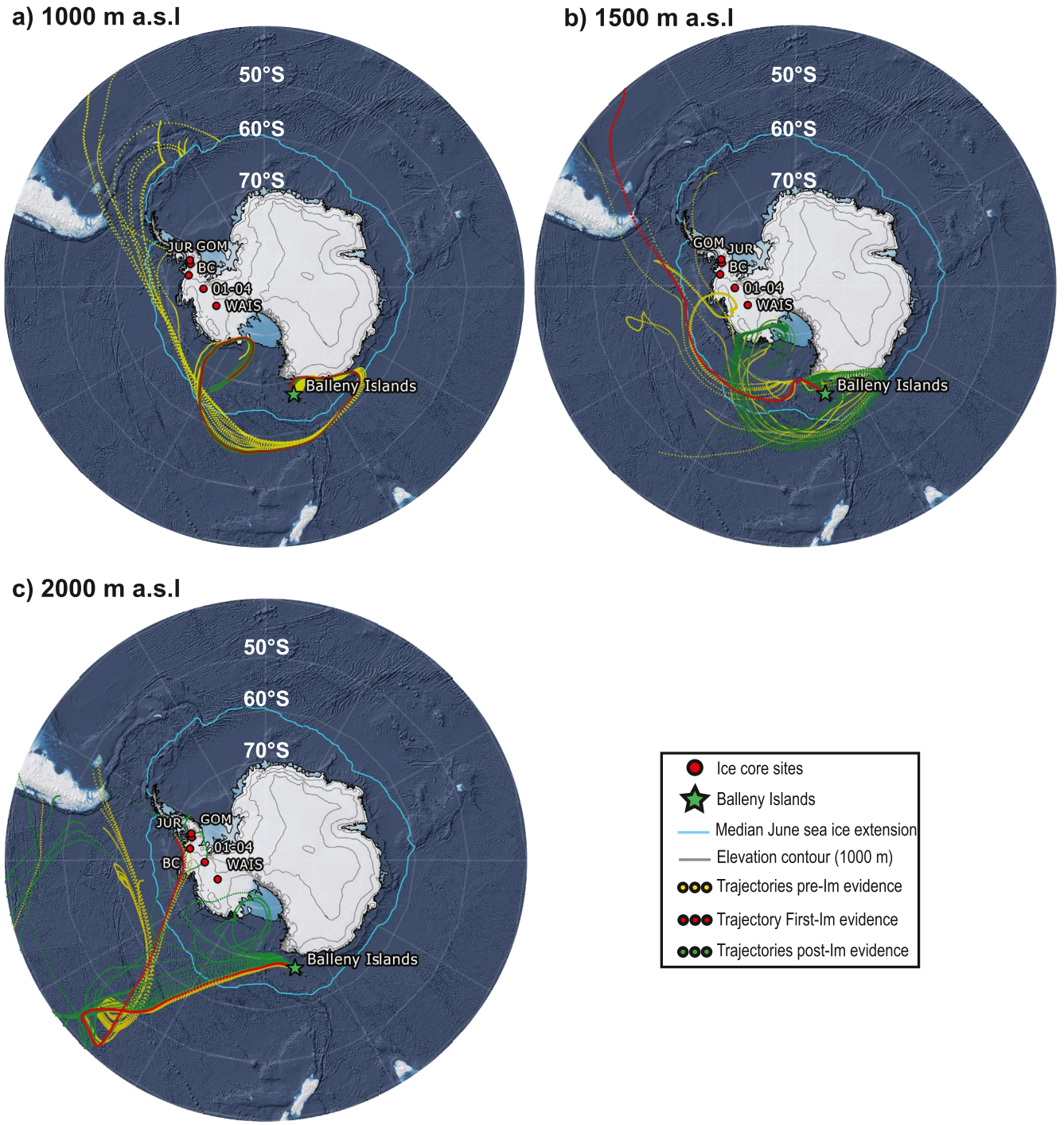

Figure 6. 10-day trajectories departing from Sturge Island on the 12 June 2001 at three different heights: (a) 1,000, (b) 1,500 ,and (c) 2,000 m a.s.l. Color coded trajectories indicate if they passed through Sturge Island before, during, or after the first image evidence of an unusual cloud formation. Median June sea ice-extension is based on 1980–2010 CE.

02:00 UTC trajectory remained within the June sea-ice zone, passing over the ice sheet in Ellsworth Land and into the southern Antarctic Peninsula. An additional group of five trajectories was identified passing near WAIS and 01-4 ice core sites at 1,500 m a.s.l. These trajectories were passing over the Balleny Islands between 08:00 and 13:00 UTC on the June 12, 2001. After leaving the Balleny Islands they were transported over the June sea-ice zone of the Amundsen Sea before reaching the Walgreen Coast in the Amundsen Sea embayment (Figure 6b).

4. Discussion

4.1. Pinatubo/Hudson (1991 CE) and El Chichón (1982 CE) Eruptions

The evaluation of previously identified volcanic eruptions, especially Pinatubo/Hudson (1991 CE) and El Chichón (1982 CE), is intended to verify the robustness of volcanic identification in the ice core sites used in this study. The 1994–1992 CE and 1984–1982 CE ice layers are distinctive periods in the ice core record. These intervals show strong similarities in the presence and consistency of prominent summer peaks above the background variability in total sulfate concentration (SO_4^{2-}), EC, and MPC. The levels of SO_4^{2-} and MPC in the two intervals are above the detection threshold, suggesting an additional input of SO_4^{2-} and microparticles during these periods. In Antarctica, the 1994–1992 CE and 1984–1982 CE ice core layers have been linked to the well-documented eruptions of Mount Pinatubo/Cerro Hudson (1991 CE; Cole-Dai & Mosley-Thompson, 1999; Hoffmann et al., 2020; Jiang et al., 2012; Osipov et al., 2014; Plummer et al., 2012; Schwanck et al., 2017; Thoen et al., 2018; Zhang et al., 2002) and El Chichón (1982 CE; Inoue et al., 2017; Jiang et al., 2012; Kohno et al., 1999; Plummer et al., 2012; Thoen et al., 2018; Traufetter et al., 2004), the two volcanic eruptions with the greatest SO_2 emissions worldwide of the 1977–2007 CE period (Shinohara, 2008). Therefore, we propose the excess of SO_4^{2-} and MPC identified during these periods (1994–1992 CE & 1984–1982 CE) were derived from the large low-latitude (mid-latitude) Pinatubo (Cerro Hudson) and El Chichón eruptions.

Subtle differences were identified in the signals of SO_4^{2-}, nss SO_4^{2-}, EC and MPC between the 1994–1992 CE and 1984–1982 CE ice core layers. The principal difference was associated with the magnitude of the SO_4^{2-}, nss SO_4^{2-}, EC and MPC peak(s) in each layer. Peaks in the 1994–1992 CE ice core layer were higher and more persistent, while peaks from the 1984–1982 CE ice layer were smaller or absent (nssSO_4^{2-}-flux). These discrepancies are explained by differences in the volumetric emissions from each eruption, classified on the logarithmic scale of the Volcanic Explosivity Index (VEI). As VEI-6 (VEI-5), the Pinatubo (Cerro Hudson) eruption released at least 10 km^3 (1 km^3) of particles and gases to the atmosphere, whilst the El Chichón VEI-5 eruption, ejected only 1 km^3. The difference in the scale of these two eruptions accounts for the different signal strengths observed in the 1994–1992 and 1984–1982 CE ice layers. Our results are consistent with observations from several Antarctic ice cores presenting a stronger signal for Pinatubo/Hudson and a weaker signal for El Chichón (Inoue et al., 2017; Plummer et al., 2012; Thoen et al., 2018).

The records identified for the Pinatubo/Hudson and El Chichón eruptions provide two examples of how different parameters measured in ice cores from the southern Antarctic Peninsula, Ellsworth Land and Marie Byrd Land can effectively record recent major low-latitude volcanic eruptions. The findings also highlight the limitations of using SO_4^{2-}, nss SO_4^{2-} in the ice core sites downwind of the Balleny islands. The high background concentrations, from adjacent oceanic sources, and influence of extreme precipitation events (Turner et al., 2019) make it difficult to identify even large volcanic eruptions clearly or consistently.

4.2. The 2001 CE Ice Core Horizon

In 2001, remote sensing observations from Sturge Island presented inconclusive evidence for recent volcanic activity in the Balleny Islands. Numerous lines of evidence from the ice core record provide independent evidence that a high-latitude volcanic eruption occurred at this time.

The 2001 ice core layer (2001L) presents some of the most striking features identified in the 1977–2007 CE period. This layer exhibited a prominent and synchronous SO_4^{2-}-EC $> 2\sigma$-peak on each ice core analyzed. Its presence in ice across Marie Byrd Land, Ellsworth Land, and the southern Antarctic Peninsula, highlights it as a persistent regional feature. Even though the $>2\sigma$ signal is only represented by a single data point in two ice core records (SO_4^{2-} in JUR and WAIS), its consistent presence across the region rules out the possibility of analytical outliers or sample contamination. The magnitude and regional distribution of the SO_4^{2-}-EC $> 2\sigma$-peaks suggest it was caused by an exceptional input of sulfates to an extended area of the ice sheet during mid-2001. Further analyses of the MSA record showed the absence of peaks during the austral autumn/winter of 2001. Thus, demonstrating the SO_4^{2-}-EC $> 2\sigma$-peak was not produced by increased austral autumn/winter marine biogenic productivity (Mulvaney et al., 1992). The lack of evidence for a biogenic source suggests the SO_4^{2-} $>2\sigma$-peak identified in the 2001 ice core layer could have been caused either by inputs from a volcanic source or by large inputs of sea salts. However, the detection of numerous cryptotephra glass shards in the mid-2001 CE ice core layer

from the JUR and GOM ice cores provides direct evidence for a volcanic eruption. Combined with the observed MPC>2σ-peak in WAIS and JUR for the 2001L, this supports the assertion that the excess SO_4^{2-} is derived from a volcanic source. The elevated inputs of SO_4^{2-} & MPC recorded in 2001L are comparable to those observed in the 1994–1992 CE and 1984–1982 CE ice core layers, attributed to Pinatubo/Hudson and El Chichón eruptions, respectively (Section 4.1).

Results from PSD analyses spatially constrain a possible source for the 2001 volcanic products. In particular, the PSD profile for the 2001 MPC > 2σ-peak presented a considerable increase in the volume and size of particles (mode diameter = 10 μm), compared with the background PSD (mode diameter = 5.7 μm). The coarser-than background PSD in 2001L suggests a more proximal volcanic source (Koffman et al., 2013) because coarser particles are unlikely to be transported large distances. Additionally, the spatial gradient identified in the VSF suggests the transport and deposition of volcanic sulfate was from the Amundsen Sea sector toward the Bellingshausen Sea sector. Thus, establishing an eastward dispersion of the volcanic cloud. Results from the PSD and the net VSF are complemented by the synchronous deposition of the SO_4^{2-}, EC, and MPC peaks that indicate rapid tropospheric transport and therefore also support a closer volcanic source (Koffman et al., 2017). Similarly, the angular texture of the cryptotephras suggests these glass shards were produced, transported, and deposited within a short interval, without being altered by reworking or weathering processes.

To date, the Global Volcanic Program list of volcanic emissions only records two major volcanic events (VEI ≥ 4) for the 1998–2001 CE period. These events correspond to Shiveluch volcano in Russia (ongoing eruption since 1999 CE, VEI = 4) and to Ulawun volcano in Papua New Guinea (September 2000 CE, VEI = 4). Additionally, during the same period, there is only one confirmed major source of SO_2 volcanic emissions, the Nyamuragira volcano in equatorial Africa (Shinohara, 2008). In the 1998–2001 CE period, the Nyamuragira volcano erupted three times: October 1998 CE, January 2000 CE, and February 2001 CE. All these eruptions presenting a VEI = 2. Despite the evidence of two major volcanic events and considerable SO_2 volcanic emissions from Nyamuragira during the 1998–2001 CE period, all these events occurred either in the equatorial region or in the northern hemisphere mid-latitudes. The distant location of these eruptions, their magnitude (VEI ≤ 4), and their timing cannot explain the synchronous SO_4^{2-}, EC and MPC peaks or the presence of coarse cryptotephra shards in the 2001L. Thus, establishing a small to moderate Antarctic eruption as the potential source of volcanic products present in the 2001 ice core layer.

Mount Erebus has been continuously active (lava lake activity) since 1972 CE (Kyle, 1994) and is the only volcano listed to have documented volcanic activity in Antarctica between 1998 and 2001 CE. The eruptions recorded during this period were of Strombolian type and did not exceed VEI = 2. There was a substantial increase in the number of eruptions per month during 1998 CE and 2000 CE. However, there was a sharp decrease in the number of eruptions after May 2000 CE, leading to the absence of eruptions between March 2001 and February 2002 (Global Volcanism Program, 2006, 2017). Despite the potential of Mount Erebus to be considered as the source to the volcanic signature in the 2001L, the relatively continuous emission from small eruptions would be represented in the ice core record as the background signal, rather than as prominent peaks. Moreover, the proximity of Mount Erebus to the ice core sites would require a small to moderate eruption to have occurred in mid-2001. However, the lack of eruptions during this period rules out the possibility of Erebus as the source of volcanic products seen in the 2001 ice core layer. Although Mount Erebus is discarded as the volcanic source, a potential small to moderate Antarctic eruption is consistent with remote sensing observations from Sturge Island on the 12 June 2001.

The analyses of air mass transport pathways provide key evidence linking remote sensing observations to the ice core record. Trajectory analyses confirm air parcels passing over Sturge Island at low elevations (1,500 and 2,000 m a.s.l) during the unusual cloud formation, were transported to the ice core sites in Ellsworth Land and southern Antarctic Peninsula within a week. The detection of a volcanic signal in the WAIS ice core, despite trajectories not passing directly over the ice core site, can be explained by the coarse resolution of the trajectory model (2.5° lat.-long.), potential mixing with neighboring air parcels (both vertically and horizontally), and/or trajectories reaching the site after the designated 10 days period. The air masses passing over Sturge Island on the 12 June 2001, likely incorporated particles and chemical compounds from the eruption cloud then carried and deposited them over Marie Byrd Land, Ellsworth Land, and the southern Antarctic Peninsula.

Sturge Island appears as a strong candidate. However, the lack of ground-based observations and inconclusive remote sensing observations prevent the confirmation of it as the unequivocal source. No published information exists for Sturge Island, which appears not to have been visited by geologists. However, the Balleny islands are entirely volcanic (Hatherton et al., 1965; Wright and Kyle, 1990). From the examination of photographs and the few published descriptions and analyses (Johnson et al., 1982), each of the islands appears to be formed from the products of multiple overlapping mafic volcanic shields. Based on the strata exposed in the cliffs forming much of the coastlines, the eruptions were predominantly effusive, although a description of tuff and 'agglomerate scoria' indicates that at least some explosive events also occurred and may have affected Sturge Island. The subdued, shield-like morphologies indicate that explosivity was probably minor in the islands, however, and probably mainly low-energy, Strombolian in character. Sturge Island rises gradually from a low cliff on its west coast to >1,000 m, then falls away in prominent cliffs that form the entire east coast. Satellite images of Sturge Island show no obvious primary volcanic landforms, which is puzzling if an explosive eruption occurred as recently as 2001 CE. However, any feature would rapidly get filled by snow. Indeed, the faint outline of a possible crater rim is present at the south end of the island, close to Cape Smyth. With a diameter of >2 km, it is relatively large and low, inconsistent with a Strombolian origin. It may therefore be hydrovolcanic, which would give greater dispersal of any tephra (J. Smellie, pers. comm). Based on the topographical features of the island, the unusual cloud formation identified on the 12 June 2001 could be interpreted either as a banner cloud or as a volcanic plume. The absence of analogous cloud features associated with nearby islands could be either explained by the effect of weather interacting with variations in the island topographies, or by a volcanic eruption occurring in Sturge Island. Either way, remote sensing evidence alone is not enough to confirm or reject a volcanic eruption.

Results presented here support the volcanic origin of the unusual cloud formation and are consistent with previous studies identifying the Balleny Islands as the source of earlier volcanic products preserved in ice cores from Marie Byrd Land (Dunbar et al., 2003; Koffman et al., 2013; Kurbatov et al., 2006). Buckle Island is suggested as the source of three cryptotephra layers deposited in 1839, 1809, and 1804 CE (Kurbatov et al., 2006). The most recent of which was confirmed by historical records from sailors who observed a volcanic plume rising from Buckle Island in 1839 CE (LeMasurier et al., 1990). This 1839 eruption was recognized in the WAIS ice core and characterized by the presence of cryptotephra in two horizons with elevated particle concentration and a considerable increase of the mode particle diameter (>10 μm) over the PSD background dust (5.1 μm; Koffman et al., 2013). Likewise, several cryptotephra layers identified in the ice core record show that Antarctic eruptions typically increase the mode particle diameter (>6 μm; Koffman et al., 2013; Narcisi et al., 2010) corresponding with elevated SO_4^{2-}-EC and MPC deposition. In addition, air mass trajectories are consistent with previous studies showing the absence of a 2001 Sturge Island eruption record in ice cores from the inland sites of Mount Johns and the Ellsworth Mountains in the West Antarctic ice sheet (Hoffmann et al., 2020; Thoen et al., 2018).

In summary, the ice core records, air mass trajectory analyses, and remote sensing observations presented here provide strong evidence that a short-lived, small to moderate volcanic eruption took place on Sturge Island in mid-2001. Evidence suggests that volcanic products from this eruption were rapidly transported through the troposphere and deposited inland over Marie Byrd Land, Ellsworth Land, and the southern Antarctic Peninsula. The deposition over the ice sheet produced a volcanically enriched layer that has been preserved in the ice core record.

The detection of this 2001 eruption may demonstrate Sturge Island is an active volcano capable of producing small-moderate explosive events. It is possible that previous eruptions recognized in Antarctic ice core records and attributed to Buckle Island, could instead, have originated from Sturge Island. If true, Sturge Island could be at least as active as Buckle Island. Thus, suggesting a reinterpretation of the Balleny Island hot-spot dynamics (Green, 1992). Additionally, the prominent and consistent volcanic signal identified in the 2001 ice core layers from Marie Byrd Land, Ellsworth Land, and the southern Antarctic Peninsula highlight this ice core horizon as a new, 21st century, chronostratigraphic marker between the eruptions of Pinatubo/Hudson (1991 CE, VEI = 6 and VEI = 5) and Puyehue-Cordon Caulle (2011 CE, VEI = 5). As such, the Sturge Island 2001 eruption provides a valuable volcanic horizon to date ice cores from the Amundsen and Bellingshausen Seas sectors.

The evidence presented in this work of a new 21st century volcanic horizon in West Antarctic ice cores supports the occurrence of a volcanic eruption in Sturge Island in 2001. Whilst geochemical analyses of the cryptotephra shards would be required to unequivocally determine the Balleny Islands as the volcanic source, the evidence presented here is sufficiently robust to assign this cryptotephra layer in ice cores as a chronostratigraphic marker.

5. Conclusions

Antarctica is one of the most enigmatic volcanic regions on Earth, with potentially hundreds of volcanoes hidden beneath the ice sheet. New historical records of active volcanism in Antarctica provide valuable information to study how volcanic activity can shape the polar climate and its potential impacts on the cryosphere. A set of ice core records from Marie Byrd Land, Ellsworth Land, and the southern Antarctic Peninsula have been analyzed to validate previous inconclusive evidence of a 2001 volcanic eruption on Sturge Island, part of the Balleny Island chain. The 2001 ice core layer contains a regional input of sulfates and microparticles, which when evaluated together, are consistent with a volcanic source. The combined presence of volcanic tephra shards, particle coarsening and in-phase deposition of potentially volcanic products indicate a small to moderate Antarctic eruption as the source and a rapid tropospheric dispersion as the transport mechanism. Air mass trajectory analyses proved air parcels passing over Sturge Island during the 2001 eruption were effectively transported, within a week, to the ice core sites.

The evidence presented here builds on previous inconclusive remote sensing observations to advocate Sturge Island as an active volcano with recent eruptive states. The regional extent of this volcanic event across several Antarctic ice core records may highlight its potential as a chronostratigraphic marker to improve the accuracy of 21st century ice chronologies. The detection of small to moderate eruptions in Antarctic ice core records is a challenging endeavor, only possible by following a multi-proxy approach. No single record can provide unequivocal evidence of a volcanic event, however, when used together they present a convincing argument. Further research should be focused on performing geochemical analyses of the cryptotephra shards to unambiguously fingerprint the volcanic source.

Conflict of Interest

The authors declare that the research was conducted in the absence of any commercial or financial relationships that could be construed as a potential conflict of interest.

Data Availability Statement

Data sets for this research are available in these in-text data citation references: Mayewski and Dixon (2005), Sigl et al. (2016), and Thomas et al. (2015, 2008). WAIS Divide data sets are available at National Snow and Ice Data Center (https://nsidc.org/data/agdc/data-wais-divide) and at the U.S. Antarctic Program Data Center (https://www.usap-dc.org/). Data sets from the ITASE 01-4 ice core are available at NASA Earth Data Common Metadata repository (https://cmr.earthdata.nasa.gov/search/concepts/C1214591464-SCIOPS). Data sets original to this work will be available at the UK Polar Data Center (https://www.bas.ac.uk/data/uk-pdc/).

Acknowledgments
The authors would like to thank Professor Christine Lane from the Geography Department, University of Cambridge, for her help with cryptotephra shard identification. The authors would like to thank Jorge Romero from the University of Manchester for his help with initial cryptotephra shard identification. The authors would like to thank Professor Eric Wolff from the Earth Sciences Department, University of Cambridge, for his comments and suggestions during the final reviewing and editing of the submitted manuscript. The authors would like to thank the Ice core Lab staff from the British Antarctic Survey, for their help while processing the Jurassic ice core. The authors highly appreciate the time and consideration of three reviewers, Professor John Smellie and two anonymous reviewers, who provided constructive comments and observations that helped improve this manuscript. The authors are also grateful to Professor John Smellie for providing the description of the geology of Sturge Island. This research was funded by CONICYT-Becas Chile and Cambridge Trust funding program for Ph.D. studies. Grant number 72180432.

References

Abram, N. J., Mulvaney, R., & Arrowsmith, C. (2011). Environmental signals in a highly resolved ice core from James Ross Island, Antarctica. *Journal of Geophysical Research: Atmospheres*, *116*(D20). https://doi.org/10.1029/2011jd016147

Abram, N. J., Mulvaney, R., Wolff, E. W., Triest, J., Kipfstuhl, S., Trusel, L. D., et al. (2013). Acceleration of snow melt in an Antarctic Peninsula ice core during the 20th century. *Nature Geoscience*, *6*(5), 404–411. https://doi.org/10.1038/ngeo1787

Abram, N. J., Thomas, E. R., McConnell, J. R., Mulvaney, R., Bracegirdle, T. J., Sime, L. C., & Aristarain, A. J. (2010). Ice core evidence for a 20th century decline of sea ice in the Bellingshausen Sea, Antarctica. *Journal of Geophysical Research: Atmospheres*, *115*(D23). https://doi.org/10.1029/2010jd014644

Aristarain, A. J., & Delmas, R. J. (1998). Ice record of a large eruption of Deception Island Volcano (Antarctica) in the XVIIth century. *Journal of Volcanology and Geothermal Research*, *80*(1–2), 17–25. https://doi.org/10.1016/s0377-0273(97)00040-1

Basile, I., Petit, J. R., Touron, S., Grousset, F. E., & Barkov, N. (2001). Volcanic layers in Antarctic (Vostok) ice cores: Source identification and atmospheric implications. *Journal of Geophysical Research: Atmospheres*, *106*(D23), 31915–31931. https://doi.org/10.1029/2000jd000102

Bingham, R. G., & Siegert, M. J. (2009). Quantifying subglacial bed roughness in Antarctica: Implications for ice-sheet dynamics and history. *Quaternary Science Reviews*, *28*(3–4), 223–236. https://doi.org/10.1016/j.quascirev.2008.10.014

Breton, D. J., Koffman, B. G., Kurbatov, A. V., Kreutz, K. J., & Hamilton, G. S. (2012). Quantifying signal dispersion in a hybrid ice core melting system. *Environmental Science & Technology*, *46*(21), 11922–11928. https://doi.org/10.1021/es302041k

Budner, D., & Cole-Dai, J. (2003). *The number and magnitude of large explosive volcanic eruptions between 904 and 1865 CE: Quantitative evidence from a new south pole ice core* (Vol. 139, pp. 165–176). Geophysical Monograph-American Geophysical Union. https://doi.org/10.1029/139gm10

Castellano, E., Becagli, S., Jouzel, J., Migliori, A., Severi, M., Steffensen, J. P., et al. (2004). Volcanic eruption frequency over the last 45 ky as recorded in Epica-Dome C ice core (East Antarctica) and its relationship with climatic changes. *Global and Planetary Change*, *42*(1–4), 195–205. https://doi.org/10.1016/j.gloplacha.2003.11.007

Cole-Dai, J. (2010). Volcanoes and climate. *Wiley Interdisciplinary Reviews: Climate Change*, *1*(6), 824–839.
Cole-Dai, J., & Mosley-Thompson, E. (1999). The Pinatubo eruption in South Pole snow and its potential value to ice-core paleovolcanic records. *Annals of Glaciology*, *29*, 99–105. https://doi.org/10.3189/172756499781821319
Cole-Dai, J., Mosley-Thompson, E., & Thompson, L. G. (1997). Annually resolved southern hemisphere volcanic history from two Antarctic ice cores. *Journal of Geophysical Research: Atmospheres*, *102*(D14), 16761–16771.
Cole-Dai, J., Mosley-Thompson, E., Wight, S. P., & Thompson, L. G. (2000). A 4,100 yr record of explosive volcanism from an East Antarctica ice core. *Journal of Geophysical Research: Atmospheres*, *105*(D19), 24431–24441.
Criscitiello, A. S., Das, S. B., Evans, M. J., Frey, K. E., Conway, H., Joughin, I., et al. (2013). Ice sheet record of recent sea-ice behavior and polynya variability in the Amundsen Sea, West Antarctica. *Journal of Geophysical Research: Oceans*, *118*(1), 118–130. https://doi.org/10.1029/2012jc008077
Curran, M. A., van Ommen, T. D., Morgan, V. I., Phillips, K. L., & Palmer, A. S. (2003). Ice core evidence for Antarctic sea ice decline since the 1950s. *Science*, *302*(5648), 1203–1206. https://doi.org/10.1126/science.1087888
de Vries, M. V. W., Bingham, R. G., & Hein, A. S. (2018). A new volcanic province: An inventory of subglacial volcanoes in West Antarctica. *Geological Society, London, Special Publications*, *461*(1), 231–248. https://doi.org/10.1144/sp461.7
Dixon, D., Mayewski, P. A., Kaspari, S., Sneed, S., & Handley, M. (2004). A 200 yr sub-annual record of sulfate in West Antarctica, from 16 ice cores. *Annals of Glaciology*, *39*, 545–556. https://doi.org/10.3189/172756404781814113
Draxler, R. R., & Hess, G. D. (1998). An overview of the HYSPLIT_4 modeling system for trajectories. *Australian Meteorological Magazine*, *47*(4), 295–308.
Dunbar, N. W., & Kurbatov, A. V. (2011). Tephrochronology of the Siple Dome ice core, West Antarctica: Correlations and sources. *Quaternary Science Reviews*, *30*(13–14), 1602–1614. https://doi.org/10.1016/j.quascirev.2011.03.015
Dunbar, N. W., Zielinski, G. A., & Voisins, D. T. (2003). Tephra layers in the Siple Dome and Taylor Dome ice cores, Antarctica: Sources and correlations. *Journal of Geophysical Research: Solid Earth*, *108*(B8). https://doi.org/10.1029/2002jb002056
Fujita, S., Parrenin, F., Severi, M., Motoyama, H., & Wolff, E. W. (2015). Volcanic synchronization of Dome Fuji and Dome C Antarctic deep ice cores over the past 216 kyr. *Climate of the Past*, *11*(10), 1395–1416. https://doi.org/10.5194/cp-11-1395-2015
Gautier, E., Savarino, J., Erbland, J., Lanciki, A., & Possenti, P. (2016). Variability of sulfate signal in ice core records based on five replicate cores. *Climate of the Past*, *12*(1), 103–113. https://doi.org/10.5194/cp-12-103-2016
Global Volcanism Program. (2001). Report on Sturge Island (Antarctica). In R. Wunderman (Ed.), *Bulletin of the Global Volcanism Network* (Vol. 26, p. 5). Smithsonian Institution. https://doi.org/10.5479/si.GVP.BGVN200105-390012
Global Volcanism Program. (2006). Report on Erebus (Antarctica). In R. Wunderman (Ed.), *Bulletin of the Global Volcanism Network* (Vol. 31, p. 12). Smithsonian Institution. https://doi.org/10.5479/si.GVP.BGVN200612-390020
Global Volcanism Program. (2017). Report on Erebus (Antarctica). In A. E. Crafford, & E. Venzke (Eds.), *Bulletin of the Global Volcanism Network* (Vol. 42, p. 6). Smithsonian Institution. https://doi.org/10.5479/si.GVP.BGVN201706-390020
Goodwin, B. P. (2013). *Recent environmental changes on the Antarctic Peninsula as recorded in an ice core from the Bruce Plateau, (Doctoral dissertation)*. The Ohio State University.
Green, T. H. (1992). Petrology and geochemistry of basaltic rocks from the Balleny Is, Antarctica. *Australian Journal of Earth Sciences*, *39*(5), 603–617. https://doi.org/10.1080/08120099208728053
Hatherton, T., Dawson, E. W., & Kinsky, F. C. (1965). Balleny Islands reconnaissance expedition. *New Zealand Journal of Geology and Geophysics*, *8*(2), 164–179. https://doi.org/10.1080/00288306.1965.10428105
Hoffmann, K., Fernandoy, F., Meyer, H., Thomas, E. R., Aliaga, M., Tetzner, D., et al. (2020). Stable water isotopes and accumulation rates in the Union Glacier region, Ellsworth Mountains, West Antarctica, over the last 35 yr. *The Cryosphere*, *14*(3), 881–904. https://doi.org/10.5194/tc-14-881-2020
Hund, A. J. (2014). *Antarctica and the Arctic circle: A Geographic Encyclopedia of the Earth's Polar Regions* (Vol. 2). ABC-CLIO.
Inoue, M., Curran, M. A., Moy, A. D., van Ommen, T. D., Fraser, A. D., Phillips, H. E., & Goodwin, I. D. (2017). A glaciochemical study of the 120 m ice core from Mill Island, East Antarctica. *Climate of the Past*, *13*(5), 437–453. https://doi.org/10.5194/cp-13-437-2017
Jiang, S., Cole-Dai, J., Li, Y., Ferris, D. G., Ma, H., An, C., et al. (2012). A detailed 2,840 yr record of explosive volcanism in a shallow ice core from Dome A, East Antarctica. *Journal of Glaciology*, *58*(207), 65–75. https://doi.org/10.3189/2012jog11j138
Jiankang, H., Zichu, X., Jiahong, W., Jiancheng, K., & Guocai, Z. (1999). *Mass balance study on Collins Ice Cap, King George Island, Antarctica: Spatial and temporal variations* (pp. 209–215). IAHS-AISH publication.
Johnson, G. L., Kyle, P. R., Vanney, J. R., & Campsie, J. (1982). Geology of Scott and Balleny Islands, Ross Sea, Antarctica, and morphology of adjacent seafloor. *New Zealand Journal of Geology and Geophysics*, *25*(4), 427–436. https://doi.org/10.1080/00288306.1982.10421508
Kittleman, L. R. (1979). Tephra. *Scientific American*, *241*(6), 160–177. https://doi.org/10.1038/scientificamerican1279-160
Koffman, B. G., Dowd, E. G., Osterberg, E. C., Ferris, D. G., Hartman, L. H., Wheatley, S. D., et al. (2017). Rapid transport of ash and sulfate from the 2011 Puyehue-Cordón Caulle (Chile) eruption to West Antarctica. *Journal of Geophysical Research: Atmospheres*, *122*(16), 8908–8920. https://doi.org/10.1002/2017jd026893
Koffman, B. G., Kreutz, K. J., Breton, D. J., Kane, E. J., Winski, D. A., Birkel, S. D., et al. (2014). Centennial-scale variability of the Southern Hemisphere westerly wind belt in the eastern Pacific over the past two millennia. *Climate of the Past*, *10*(3), 1125–1144. https://doi.org/10.5194/cp-10-1125-2014
Koffman, B. G., Kreutz, K. J., Kurbatov, A. V., & Dunbar, N. W. (2013). Impact of known local and tropical volcanic eruptions of the past millennium on the WAIS Divide microparticle record. *Geophysical Research Letters*, *40*(17), 4712–4716. https://doi.org/10.1002/grl.50822
Kohno, M., Fujii, Y., Kusakabe, M., & Fukuoka, T. (1999). The last 300 yr volcanic signals recorded in an ice core from site H15, Antarctica. *Journal of the Japanese Society of Snow and Ice*, *61*(1), 13–24. https://doi.org/10.5331/seppyo.61.13
Kreutz, K. J., Koffman, B. G. (2015). *"WAIS Divide Microparticle Concentration and Size Distribution, 0–2,400 ka"*. U.S. Antarctic Program (USAP) Data Center. https://doi.org/10.7265/N5KK98QZ
Kreutz, K. J., Kurbatov, A. V., Wells, M., & Mayewski, P. A. (2011). *COLLABORATIVE RESEARCH: Microparticle/tephra analysis of the WAIS Divide ice core*. National Science Foundation.
Kreutz, K. J., & Mayewski, P. A. (1999). Spatial variability of Antarctic surface snow glaciochemistry: Implications for palaeoatmospheric circulation reconstructions. *Antarctic Science*, *11*(1), 105–118. https://doi.org/10.1017/s0954102099000140
Kreutz, K. J., Mayewski, P. A., Pittalwala, I. I., Meeker, L. D., Twickler, M. S., & Whitlow, S. I. (2000). Sea level pressure variability in the Amundsen Sea region inferred from a West Antarctic glaciochemical record. *Journal of Geophysical Research: Atmospheres*, *105*(D3). https://doi.org/10.1029/1999jd901069

Kurbatov, A. V., Zielinski, G. A., Dunbar, N. W., Mayewski, P. A., Meyerson, E. A., Sneed, S. B., & Taylor, K. C. (2006). A 12,000 yr record of explosive volcanism in the Siple Dome Ice Core, West Antarctica. *Journal of Geophysical Research: Atmospheres*, *111*(D12). https://doi.org/10.1029/2005jd006072

Kyle, P. R. (1994). *Volcanological and environmental studies of Mount Erebus, Antarctica*. American Geophysical Union.

Lee, J. E., Brook, E. J., Bertler, N. A. N., Buizert, C., Baisden, T., Blunier, T., et al. (2020). An 83,000 yr oldice core from Roosevelt Island, Ross Sea, Antarctica. *Climate of the Past*, *16*(5), 1691–1713. https://doi.org/10.5194/cp-16-1691-2020

LeMasurier, W. E., Thomson, J. W., Baker, P. E., Kyle, P. R., Rowley, P. D., Smellie, J. L., & Verwoerd, W. J. (1990). *Volcanoes of the Antarctic Plate and Southern Ocean* (Vol. 48). American Geophysical Union.

Li, C., Xiao, C., Hou, S., Ren, J., Ding, M., & Guo, R. (2012). Dating a 109.9 m ice core from Dome A (East Antarctica) with volcanic records and a firn densification model. *Science China Earth Sciences*, *55*(8), 1280–1288. https://doi.org/10.1007/s11430-012-4393-4

Maupetit, F., & Delmas, R. J. (1992). Chemical composition of falling snow at Dumont d'Urville, Antarctica. *Journal of Atmospheric Chemistry*, *14*(1–4), 31–42. https://doi.org/10.1007/bf00115220

Mayewski, P. A., & Dixon, D. A. (2005). *US International Trans Antarctic Scientific Expedition (US ITASE) glaciochemical data*. National Snow and Ice Data CenterDigital Media.

Mulvaney, R. (2013). Ice core methods, conductivity studies. In *Encyclopedia of Quaternary Science* (pp. 319–325). Elsevier. https://doi.org/10.1016/b978-0-444-53643-3.00311-3

Mulvaney, R., Abram, N. J., Hindmarsh, R. C. A., Arrowsmith, C., Fleet, L., Triest, J., et al. (2012). Recent Antarctic Peninsula warming relative to Holocene climate and ice-shelf history. *Nature*, *489*(7414), 141–144. https://doi.org/10.1038/nature11391

Mulvaney, R., Pasteur, E. C., Peel, D. A., Saltzman, E. S., & WHUNG, P. Y. (1992). The ratio of MSA to non-sea-salt sulphate in Antarctic Peninsula ice cores. *Tellus B: Chemical and Physical Meteorology*, *44*(4), 295–303. https://doi.org/10.1034/j.1600-0889.1992.t01-2-00007.x

Narcisi, B., Petit, J. R., & Delmonte, B. (2010). Extended East Antarctic ice-core tephrostratigraphy. *Quaternary Science Reviews*, *29*(1–2), 21–27. https://doi.org/10.1016/j.quascirev.2009.07.009

Narcisi, B., Petit, J. R., Delmonte, B., Basile-Doelsch, I., & Maggi, V. (2005). Characteristics and sources of tephra layers in the EPICA-Dome C ice record (East Antarctica): Implications for past atmospheric circulation and ice core stratigraphic correlations. *Earth and Planetary Science Letters*, *239*(3–4), 253–265. https://doi.org/10.1016/j.epsl.2005.09.005

Narcisi, B., Petit, J. R., Delmonte, B., Batanova, V., & Savarino, J. (2019). Multiple sources for tephra from CE 1259 volcanic signal in Antarctic ice cores. *Quaternary Science Reviews*, *210*, 164–174. https://doi.org/10.1016/j.quascirev.2019.03.005

Narcisi, B., Petit, J. R., Delmonte, B., Scarchilli, C., & Stenni, B. (2012). A 16,000 yr tephra framework for the Antarctic ice sheet: A contribution from the new Talos Dome core. *Quaternary Science Reviews*, *49*, 52–63. https://doi.org/10.1016/j.quascirev.2012.06.011

Narcisi, B., Petit, J. R., Langone, A., & Stenni, B. (2016). A new Eemian record of Antarctic tephra layers retrieved from the Talos Dome ice core (Northern Victoria Land). *Global and Planetary Change*, *137*, 69–78. https://doi.org/10.1016/j.gloplacha.2015.12.016

Nardin, R., Amore, A., Becagli, S., Caiazzo, L., Frezzotti, M., Severi, M., et al. (2020). Volcanic fluxes over the last millennium as recorded in the Gv7 Ice Core (Northern Victoria Land, Antarctica). *Geosciences*, *10*(1), 38. https://doi.org/10.3390/geosciences10010038

Osipov, E. Y., Khodzher, T. V., Golobokova, L. P., Onischuk, N. A., Lipenkov, V. Y., Ekaykin, A. A., et al. (2014). High-resolution 900 yr volcanic and climatic record from the Vostok area, East Antarctica. *The Cryosphere*, *8*(3), 843–851. https://doi.org/10.5194/tc-8-843-2014

Palais, J. M. (1985). Particle morphology, composition and associated ice chemistry of tephra layers in the Byrd ice core: Evidence for hydrovolcanic eruptions. *Annals of Glaciology*, *7*, 42–48. https://doi.org/10.3189/s0260305500005887

Parrenin, F., Barker, S., Blunier, T., Chappellaz, J., Jouzel, J., Landais, A., et al. (2012). On the gas-ice depth difference (Δdepth) along the EPICA Dome C ice core. *Climate of the Past*, *8*(4), 1239–1255. https://doi.org/10.5194/cp-8-1239-2012

Patrick, M. R., & Smellie, J. L. (2013). Synthesis A spaceborne inventory of volcanic activity in Antarctica and southern oceans, 2000–10. *Antarctic Science*, *25*(4), 475–500. https://doi.org/10.1017/s0954102013000436

Plummer, C. T., Curran, M. A. J., van Ommen, T. D., Rasmussen, S. O., Moy, A. D., Vance, T. R., et al. (2012). An independently dated 2,000 yr volcanic record from Law Dome, East Antarctica, including a new perspective on the dating of the 1450s CE eruption of Kuwae, Vanuatu. *Climate of the Past*, *8*(6), 1929–1940. https://doi.org/10.5194/cp-8-1929-2012

Ren, J., Li, C., Hou, S., Xiao, C., Qin, D., Li, Y., & Ding, M. (2010). A 2,680 yr volcanic record from the DT-401 East Antarctic ice core. *Journal of Geophysical Research: Atmospheres*, *115*(D11). https://doi.org/10.1029/2009jd012892

Robock, A. (2000). Volcanic eruptions and climate. *Reviews of Geophysics*, *38*(2), 191–219. https://doi.org/10.1029/1998rg000054

Röthlisberger, R., Bigler, M., Hutterli, M., Sommer, S., Stauffer, B., Junghans, H. G., & Wagenbach, D. (2000). Technique for continuous high-resolution analysis of trace substances in firn and ice cores. *Environmental Science & Technology*, *34*(2), 338–342.

Ruth, U., Wagenbach, D., Steffensen, J. P., & Bigler, M. (2003). Continuous record of microparticle concentration and size distribution in the central Greenland NGRIP ice core during the last glacial period. *Journal of Geophysical Research: Atmospheres*, *108*(D3). https://doi.org/10.1029/2002jd002376

Schwanck, F., Simões, J. C., Handley, M., Mayewski, P. A., Auger, J. D., Bernardo, R. T., & Aquino, F. E. (2017). A 125 yr record of climate and chemistry variability at the Pine Island Glacier ice divide, Antarctica. *The Cryosphere*, *11*(4), 1537–1552. https://doi.org/10.5194/tc-11-1537-2017

Severi, M., Udisti, R., Becagli, S., Stenni, B., & Traversi, R. (2012). Volcanic synchronization of the EPICA-DC and TALDICE ice cores for the last 42 kyr BP. *Climate of the Past*, *8*(2), 509–517. https://doi.org/10.5194/cp-8-509-2012

Shinohara, H. (2008). Excess degassing from volcanoes and its role on eruptive and intrusive activity. *Reviews of Geophysics*, *46*(4). https://doi.org/10.1029/2007rg000244

Sigl, M., Fudge, T. J., Winstrup, M., Cole-Dai, J., Ferris, D., McConnell, J. R., et al. (2016). The WAIS Divide deep ice core WD2014 chronology—Part 2: Annual-layer counting (0–31 ka BP). *Climate of the Past*, *12*(3), 769–786. https://doi.org/10.5194/cp-12-769-2016

Sigl, M., McConnell, J. R., Toohey, M., Curran, M., Das, S. B., Edwards, R., et al. (2014). Insights from Antarctica on volcanic forcing during the Common Era. *Nature Climate Change*, *4*(8), 693–697. https://doi.org/10.1038/nclimate2293

Smellie, J. L., Panter, K. S., & Geyer, A. (2021). *Introduction to volcanism in Antarctica: 200 million years of subduction, rifting, and continental break-up*. Geological Society.

Stein, A. F., Draxler, R. R., Rolph, G. D., Stunder, B. J., Cohen, M. D., & Ngan, F. (2015). NOAA's HYSPLIT atmospheric transport and dispersion modeling system. *Bulletin of the American Meteorological Society*, *96*(12), 2059–2077. https://doi.org/10.1175/bams-d-14-00110.1

Tetzner, D., Thomas, E. R., Allen, C. S., & Wolff, E. W. (2021). A refined method to analyze insoluble particulate matter in ice cores, and its application to diatom sampling in the Antarctic Peninsula. *Frontiers in Earth Science*, *9*, 20. https://doi.org/10.3389/feart.2021.617043

Thoen, I. U., Simões, J. C., Lindau, F. G. L., & Sneed, S. B. (2018). Ionic content in an ice core from the West Antarctic ice sheet: 1882–2008 CE. *Brazilian Journal of Geology*, *48*(4), 853–865. https://doi.org/10.1590/2317-4889201820180037

Thomas, E. R., & Abram, N. J. (2016). Ice core reconstruction of sea ice change in the Amundsen-Ross Seas since 1702 CE. *Geophysical Research Letters*, *43*(10), 5309–5317. https://doi.org/10.1002/2016gl068130

Thomas, E. R., Hosking, J. S., Tuckwell, R. R., Warren, R. A., & Ludlow, E. C. (2015). Twentieth century increase in snowfall in coastal West Antarctica. *Geophysical Research Letters*, *42*(21), 9387–9393. https://doi.org/10.1002/2015gl065750

Thomas, E. R., Marshall, G. J., & McConnell, J. R. (2008). A doubling in snow accumulation in the western Antarctic Peninsula since 1850. *Geophysical Research Letters*, *35*(1). https://doi.org/10.1029/2007gl032529

Traufetter, F., Oerter, H., Fischer, H., Weller, R., & Miller, H. (2004). Spatio-temporal variability in volcanic sulfate deposition over the past 2 kyr in snow pits and firn cores from Amundsenisen, Antarctica. *Journal of Glaciology*, *50*(168), 137–146. https://doi.org/10.3189/172756504781830222

Traversi, R., Becagli, S., Castellano, E., Migliori, A., Severi, M., & Udisti, R. (2002). High-resolution fast ion chromatography (FIC) measurements of chloride, nitrate, and sulfate along the EPICA Dome C ice core. *Annals of Glaciology*, *35*, 291–298. https://doi.org/10.3189/172756402781816564

Turner, J., Phillips, T., Thamban, M., Rahaman, W., Marshall, G. J., Wille, J. D., et al. (2019). The dominant role of extreme precipitation events in Antarctic snowfall variability. *Geophysical Research Letters*, *46*(6), 3502–3511. https://doi.org/10.1029/2018gl081517

Udisti, R., Becagli, S., Castellano, E., Mulvaney, R., Schwander, J., Torcini, S., & Wolff, E. (2000). Holocene electrical and chemical measurements from the EPICA-Dome C ice core. *Annals of Glaciology*, *30*, 20–26. https://doi.org/10.3189/172756400781820750

Vogel, S. W., Tulaczyk, S., Carter, S., Renne, P., Turrin, B., & Grunow, A. (2006). Geologic constraints on the existence and distribution of West Antarctic subglacial volcanism. *Geophysical Research Letters*, *33*(23). https://doi.org/10.1029/2006gl027344

Wagenbach, D., Ducroz, F., Mulvaney, R., Keck, L., Minikin, A., Legrand, M., et al. (1998). Sea-salt aerosol in coastal Antarctic regions. *Journal of Geophysical Research: Atmospheres*, *103*(D9), 10961–10974. https://doi.org/10.1029/97jd01804

Wright, A. C., & Kyle, P. R. (1990). Balleny Islands. In W. E. LeMasurier, & W. Thomson (Eds.), *Volcanoes of the Antarctic Plate and Southern Ocean* (Vol. 48, pp. 449–451). Antarctic Research Series.

Zhang, M. J., Li, Z. Q., Xiao, C. D., Qin, D. H., Yang, H. A., Kang, J. C., & Li, J. (2002). A continuous 250 yr record of volcanic activity from Princess Elizabeth Land, East Antarctica. *Antarctic Science*, *14*(1), 55–60. https://doi.org/10.1017/s0954102002000573